

University of Windsor

Scholarship at UWindor

Electronic Theses and Dissertations

Theses, Dissertations, and Major Papers

1982

A microscopical characterization of normal and vitamin A acid treated hairless mouse skin.

Kenneth Wayne. Baker
University of Windsor

Follow this and additional works at: <https://scholar.uwindsor.ca/etd>

Recommended Citation

Baker, Kenneth Wayne., "A microscopical characterization of normal and vitamin A acid treated hairless mouse skin." (1982). *Electronic Theses and Dissertations*. 662.
<https://scholar.uwindsor.ca/etd/662>

This online database contains the full-text of PhD dissertations and Masters' theses of University of Windsor students from 1954 forward. These documents are made available for personal study and research purposes only, in accordance with the Canadian Copyright Act and the Creative Commons license—CC BY-NC-ND (Attribution, Non-Commercial, No Derivative Works). Under this license, works must always be attributed to the copyright holder (original author), cannot be used for any commercial purposes, and may not be altered. Any other use would require the permission of the copyright holder. Students may inquire about withdrawing their dissertation and/or thesis from this database. For additional inquiries, please contact the repository administrator via email (scholarship@uwindsor.ca) or by telephone at 519-253-3000ext. 3208.

CANADIAN THESES ON MICROFICHE

I.S.B.N.

THESES CANADIENNES SUR MICROFICHE



National Library of Canada
Collections Development Branch

Canadian Theses on
Microfiche Service

Ottawa, Canada
K1A 0N4

Bibliothèque nationale du Canada
Direction du développement des collections

Service des thèses canadiennes
sur microfiche

NOTICE

The quality of this microfiche is heavily dependent upon the quality of the original thesis submitted for microfilming. Every effort has been made to ensure the highest quality of reproduction possible.

If pages are missing, contact the university which granted the degree.

Some pages may have indistinct print especially if the original pages were typed with a poor typewriter ribbon or if the university sent us a poor photocopy.

Previously copyrighted materials (journal articles, published tests, etc.) are not filmed.

Reproduction in full or in part of this film is governed by the Canadian Copyright Act, R.S.C. 1970, c. C-30. Please read the authorization forms which accompany this thesis.

THIS DISSERTATION
HAS BEEN MICROFILMED
EXACTLY AS RECEIVED

AVIS

La qualité de cette microfiche dépend grandement de la qualité de la thèse soumise au microfilmage. Nous avons tout fait pour assurer une qualité supérieure de reproduction.

S'il manque des pages, veuillez communiquer avec l'université qui a conféré le grade.

La qualité d'impression de certaines pages peut laisser à désirer, surtout si les pages originales ont été dactylographiées à l'aide d'un ruban usé ou si l'université nous a fait parvenir une photocopie de mauvaise qualité.

Les documents qui font déjà l'objet d'un droit d'auteur (articles de revue, examens publiés, etc.) ne sont pas microfilmés.

La reproduction, même partielle, de ce microfilm est soumise à la Loi canadienne sur le droit d'auteur, SRC 1970, c. C-30. Veuillez prendre connaissance des formules d'autorisation qui accompagnent cette thèse.

LA THÈSE A ÉTÉ
MICROFILMÉE TELLE QUE
NOUS L'AVONS REÇUE

A MICROSCOPICAL CHARACTERIZATION OF NORMAL
AND VITAMIN A ACID TREATED
HAIRLESS MOUSE SKIN

by



KENNETH WAYNE BAKER

A Thesis

submitted to the Faculty of Graduate Studies
through the Department of
Biology in Partial Fulfillment
of the requirements for the Degree
of Master of Science at
The University of Windsor.

Windsor, Ontario, Canada

1982

©

Kenneth Wayne Baker 1982.
All Rights Reserved

774685

ABSTRACT

This study has focused upon two principal areas of concern:

- (1) The establishment of a well characterized epidermal control system for the comparative analysis of cellular and subcellular morphological changes in hairless mouse epidermis.
- (2) The comparative morphological evaluation of epidermal responses to the prolonged application of vitamin A acid (retinoic acid).

The structural organization of normal and retinoic acid treated hairless mouse skin was evaluated with light and electron microscopic techniques. An unusual perspective was provided by the preliminary separation of the intact epidermal sheet from it's underlying dermis using 20 mM ethylene diamine tetraacetic acid (EDTA); this allowed scanning electron microscopic observation of the inferior epidermal surface (stratum basale, Langerhans cells and hairfollicles) and the superior dermal surface (basal lamina). Whole and EDTA-separated samples were also correlatively examined in cross-section using transmission

electron and light microscopy. An even distribution of hair follicles were degenerative yet possessed active sebaceous glands. In all other respects, hairless mouse epidermis was similar, in structure and organization, to the epidermis of mice with hair. An abundance of protruding Langerhans cells was a particularly prominent feature in EDTA-separated epidermal sheets; their distribution paralleled that observed in adenosine triphosphatase stained sheets.

Topical retinoic acid--known to effect a variety of physiologic and therapeutic epidermal changes--was applied to the backs of hairless mice in concentrations of 0.3% or 1.0% in a propylene glycol vehicle. Mice were treated daily for up to 14 days. Epidermal changes were of a predominately irritant nature: membrane vesicle release in EDTA-separated epidermis, synthesis of lipid, glycogen and intramitochondrial inclusions, intercellular edema and parakeratinization by 3 days exposure. Retinoic acid induced changes were substantially reduced after more prolonged treatment (14 days) and had disappeared within 2 weeks of treatment termination. Protruding Langerhans cells were no longer visible on the inferior surface of EDTA-separated epidermis during peak levels of parakeratinization (3-8 days), though they were observed in cross-section at higher levels amongst the cells in the stratum spinosum.

Clearly, the skin of the hairless mouse is an extraordinary dermatological model and, with such an

abundance of externally available, ultrastructurally sound Langerhans cells, may prove significant in the provision of new information concerning Langerhans cell function and character. In the meantime however, using this same system, topical treatment with retinoic acid has elicited an epidermal irritant response of such magnitude that specific changes solely attributable to retinoic acid are largely obscured.

DEDICATION

This thesis is dedicated
to the memory of
Mark Lawrence

ACKNOWLEDGMENTS

The author wishes to acknowledge the following for their assistance and support:

Drs. N. F. Taylor and D. A. Cotter for their assistance in the preparation and evaluation of this thesis.

Archie Glasgow, who has given generously of his time and expertise. Archie has been one of my most enlightening teachers.

John Robinson for his assistance with the scanning electron microscope.

Dr. G. C. Budd at the Medical College of Ohio, for his inspiration and technical assistance.

Dr. Geoff Rowden at Loyola University, Chicago, who first introduced me to the Langerhans cell. Dr. Rowdens support and enthusiasm have been invaluable in the completion of this work.

Bill Brown, who provided such an admirable example of initiative and hard work, and who made the pursuit of this degree a considerably easier task.

Dr. Hugh Fackrell who has supported me throughout my university career. Dr. Fackrell has also kindly provided the facilities for the typing of this manuscript.

Dr. J. E. J. Habowsky who has been my advisor and

co-worker for several years now. Dr. Habowsky has provided me with considerable financial and moral support and has been the key to the success of this thesis.

And finally, my parents, for their continuing trust and confidence.

TABLE OF CONTENTS

ABSTRACT	i
DEDICATION	iv
ACKNOWLEDGEMENTS	v
INTRODUCTION	1
General	
Hairless Mouse Skin	
Ethylene Diamine Tetraacetic Acid (EDTA)	
Ruthenium Red	
Propylene Glycol	
Retinoic Acid	
MATERIALS AND METHODS	16
Hairless Mice	
Retinoic Acid Treatment	
Tissue Processing	
EDTA Separation	
Adenosine Triphosphatase	
Light Microscopy	
Electron Microscopy	
Tissue Processing (Flow Chart)	
RESULTS	21
Microscopic Morphology and Organization in the Skin	
of the Hairless Mouse	21
Light Microscopy	
Whole Skin	
EDTA-separated Epidermis and Dermis	
Transmission Electron Microscopy	
Whole Skin	
EDTA-separated Epidermis and Dermis	
Scanning Electron Microscopy	
EDTA-separated Epidermis and Dermis	
The Epidermal Effects of Topically Applied Retinoic	
Acid	31
Transmission Electron Microscopy	
Whole Skin	
EDTA-separated Epidermis-O ₃ O ₄ Fixation	
EDTA-separated Epidermis-RR Fixation	
Scanning Electron Microscopy	
EDTA-separated Epidermis	
EDTA-separated Dermis	

Figures (1 through 44)	44-89
DISCUSSION	90
General Retinoic Acid	
APPENDICES	108
REFERENCES	112
VITA AUCTORIS	127

LIST OF ABBREVIATIONS

EDTA	-	ethylene diamine tetraacetic acid
EGTA	-	ethylene guanine tetraacetic acid
RA	-	retinoic acid
R	-	retinol
RBP	-	retinol binding protein
cRBP	-	cellular retinol binding protein
cRABP	-	cellular retinoic acid binding protein
GDP	-	guanosine diphosphate
MRP	-	mannosyl-retinyl-phosphate
LM	-	light microscopy
SEM	-	scanning electron microscopy
TEM	-	transmission electron microscopy
LC	-	Langerhans cell
LG	-	Langerhans granule
RER	-	rough endoplasmic reticulum
Ia	-	immune region associated antigen
PG	-	propylene glycol
OsO ₄	-	osmium tetroxide
RR	-	ruthenium red
PBS	-	phosphate buffered saline
IMI	-	intramitochondrial inclusions
DNCB	-	dinitrochlorobenzene

INTRODUCTION

General

The present study was undertaken to evaluate the cytologic and ultrastructural changes occurring in the epidermis of the hairless mouse after prolonged topical application of vitamin A acid (RA) in a propylene glycol vehicle.

Pre-eminent was the need for an understanding of the cytology and ultrastructure of normal, untreated hairless mouse skin. The whole skin of the hairless mouse has therefore, been studied by light (LM) and transmission electron (TEM) microscopy. Concurrently, the basal epidermal undersurface and it's dermal counterpart (including the overlying basal lamina) were isolated by chemical dissection and correlatively examined by LM, TEM, and scanning electron (SEM) microscopy. This basic control study--originally looked upon as reference material for discussion of RA induced change--has expanded in scope and is now a primary focus of this project.

The working hypothesis, in this thesis, is that epidermal changes elicited by topical exposure to pharmacological concentrations of RA are best recognized when compared with a well defined control system. RA changes, when evaluated in this context, will serve to

further characterize the nature of both physiological and therapeutic stimulus-response mechanisms. Moreover, a well characterized control system will continue to provide a basis for a variety of subsequent investigations.

Hairless Mouse Skin

Hairless mice, as used in this study, were first described by Brookes in 1926 after a pair were captured in a London aviary and successfully bred (1).

The character hairlessness is a single factor recessive condition (hr/hr) which causes reduced viability, partial sterility, and essentially complete loss of hair within three weeks of birth (1,2,3). Hair follicles are histologically normal during anagen, the growth phase, but show abnormalities during catagen, the transitional stage between anagen and the resting phase, télogen (2,3). The germinal hairs are left isolated in the dermis, incapable of reproducing a second pelage; thus, the adult mouse is totally denuded except for the vibrissae, which remain normal.

Well suited to a variety of in vivo dermatologic studies, hairless mouse epidermis is easily accessible for topical treatment and subsequent isolation and observation; these characteristics are shared only by the similarly glabrous skin of humans.

The epidermal compartment is relatively thin (5-7 cells in the live cell layers and 8-10 cells in the stratum

corneum), lacks dermal papillae and mature hairfollicles, and, possesses clearly delineated cell layers representing the progressive stages in keratinocyte differentiation and exfoliation (2,4). In addition to the large keratinocyte population, are smaller subpopulations of dendritic Langerhans cells (LCs), indeterminate cells, Merkel cells and melanocytes. Polymorphonuclear leukocytes, T-lymphocytes, and macrophages are also occasionally observed, usually in response to wounding or external antigen stimulation.

The intra-epidermal LC population is evenly distributed throughout the orthokeratinizing epithelia and forms a reticular network between and just above the basal germinativum, as compared with a supra-basal location in the epidermis of man (5) and guinea pig (6) and mouse footpad (7). Morphologically, LCs may possess up to 12 dendrites per cell and usually display a relatively clear cytoplasm with an indented nucleus (see review, 8). Tennis racquet shaped Langerhans granules (or Birbeck granules), a cytoplasm devoid of tonofilaments, and an absence of desmosomal associations with surrounding keratinocytes are, in combination, a means of conclusively identifying LCs by TEM (5,9,10). Commonly observed cytoplasmic figures are: a well developed Golgi apparatus, numerous mitochondria, an active rough endoplasmic reticulum (RER), many small vesicles, and loosely arranged 70-80 Å filaments. LCs can be observed in

both the LM and TEM using gold chloride staining (11), adenosine triphosphatase staining (7,12), or labeled antibody techniques specific for LC surface components; LCs possess membrane Ia (immune region associated) antigens (13,14,15,16), OKT6 antigens (17), C3 complement and Fc-IgG receptors (18).

LC are capable of intra-epidermal reproduction (19,20), although their true origins are from stem cells present in the bone marrow during early embryonic development (21,22). Functionally, the LC is closely linked to cells of the monocyte-macrophage-histiocyte lineage (see review, 8) and is often referred to as an epidermal macrophage regardless of its poor phagocytic capability. It is, in fact, the only cell type capable of replacing the macrophage in its role as a mediator of cellular immunity (23,24,25). Thus, the LC forms a "reticulo-epithelial system", analogous to the "reticulo-endothelial" macrophage system observed in the spleen (26). The epidermis, as such, represents the outermost organ of the mammalian immune system.

Indeterminate dendritic cells, also frequently observed in hairless mouse epidermis (4,9), closely resemble LCs in morphology yet lack the classic identifying marker, the Langerhans granule (LG). The apparent lack of such a granule results in the cell being termed as an "indeterminate cell", often with the end result that specific functional attributes are discussed with much ambiguity. Recently though, it has been demonstrated that the indeterminate cell

expresses Ia surface antigen (27), evidence clearly supporting the concept of LC-indeterminate cell quality. On the basis of this finding, and because no evidence exists to the contrary, all subsequent discussion in the present study will refer to both cell types as LCs.

Melanocytes are not observed in the dorsal trunk epidermis of hairless mice (9) or mice with hair (28), but may appear in response to carcinogen exposure (9) or, ultraviolet radiation (29).

Merkel cells are thought to represent the outermost expression of the sensory nervous system (30,31). They are closely associated with afferent nerve endings in the dermis, and basal epidermis, and possess round dense granules accumulated in the cytoplasm adjacent to the point of membrane association with contiguous nerve endings (30,31). Merkel cells are very rarely observed in the dorsal trunk epidermis as they are most commonly associated with areas of touch, such as the snout, vibrissae, and footpads (30,31).

Because it's a naturally simplified example of mammalian epidermis in general, the hairless mouse offers a unique potential as an experimental model. The thinness of the epidermal compartment, the exclusion of melanocytes, and the absence of externally active hairfollicles, reduces the system to a relatively simple presentation of LCs embedded in a matrix of actively keratinizing epithelial cells. The present study seeks to elaborate upon the nature of this

epidermal model as it exists normally, after chemical dissection with ethylene diamine tetraacetic acid (EDTA), and after prolonged topical application of RA. In this manner, the uniquely and desirable qualities of the hairless mouse as a dermatological model--with special reference to the LC--will be well illustrated and possibly recommended.

EDTA Separation

EDTA is a well known chelating agent with an affinity for calcium two orders of magnitude greater than for magnesium (32). It has been used in previous studies to chemically dissect the skin of mammals by removal of divalent cations at the dermo-epidermal junction (7,33,34). Mg^{++} , as compared to Ca^{++} , is considered to be a more effective crosslinking agent in epidermal attachment to the dermal substratum; EGTA, with an affinity for Ca^{++} six times greater than for Mg^{++} , was less effective than EDTA in epidermal separation (33).

The association of epidermis and dermis is principally mediated by divalent cations present at the filamentous point of association between basal cell hemidesmosomes and the anchoring fibrils of the dermis (33). Dermal, and epidermal polyanionic glycoproteins, in the absence of cation crosslinking, are permitted to slide past one another, thereby facilitating a clean separation of dermis and epidermis (33). This rationale is supported by microscopic observations of relatively long filamentous

7

regions located just beneath the separated hemidesmosome (7,33). The actual point of separation occurs in the "lamina lucida", the clear zone which appears between the basal lamina and the overlying basal cell (35), plasma membrane (7,33).

The basal lamina (and all underlying structures) remain undamaged after EDTA separation. The corresponding epidermis however, exhibits marginal widening of the basal intercellular space and occasional cytoplasmic engulfment of hemidesmosomes.

EDTA separation is a prerequisite to enzyme staining, reactions with isolated epidermal sheets (7,36). Moreover, it permits direct 3 dimensional visualization (using SEM) of those subcellular structures normally associated with the dermo-epidermal junction. In the present study, EDTA separation of RA treated and untreated epidermal sheets, precedes both ATPase staining of intra-epidermal LCs, and fixation for correlative microscopic examination.

Ruthenium Red

Ruthenium red (RR), an inorganic dye with a molecular size of 1.13nm (37), has been utilized in microscopy for three different yet integrable purposes: (a) as a specific stain for cell surface glycoproteins, and in some cases, intracellular glycoprotein (38); (b) complexed with OsO₄, it provides an electrically conductive surface in biological tissues, thereby allowing direct SEM visualization in the

absence of external metal coatings (39); (c) because of its large molecular size, intracellular penetration or exclusion of RR is used as an indicator of cell viability (40). In the present study, all three areas of utilization have been incorporated as a means of elaborating upon the subcellular nature of treated and untreated epidermis, before and after EDTA separation.

Propylene Glycol

Propylene glycol (1,2-propanediol, PG) is a non-toxic solvent used commonly--by itself, or in a variety of cream and liquid preparations--as a vehicle for many lipid soluble compounds (41), especially therapeutic corticosteroid preparations (42,43,44). PG can also serve as a source of carbohydrate when metabolized to its intermediate oxidation products, lactic and pyruvic acid (41). Recent studies in this laboratory have shown no gross, or microscopic changes in epidermis treated topically with unmedicated PG (45).

PG offers many advantages in the percutaneous delivery of RA: it's easily applied, readily solubilizes RA, elevates local skin temperatures and hydrates the upper levels of the epidermis (41,42,43,44). Once applied, the RA-PG is resistant to the evaporation encountered so frequently with more polar solvents such as acetone or ethanol. PG, as a vehicle, ensures a more prolonged exposure to RA while simultaneously improving its percutaneous penetration.

Retinoic Acid (Vitamin A Acid)

Vitamin A is a generic term referring to compounds, other than the carotenoids, that qualitatively exhibit retinol-like biological activity (46). Fat soluble retinol is a well known requirement for the promotion of normal growth and the general health of highly differentiated organisms (47,48,49,50,51). It's functions include essential roles in: the visual cycle, epithelial development, epithelial maintenance, mucous secretion, and reproduction (46,49,51). In comparison, retinoic acid (RA) -a well known natural metabolite of retinol (R) (52)- cannot support visual (53) or reproductive functions (46,49) in mammals, but can support bone growth, and is more effective than R in sustaining normal epithelial growth patterns (46,49,52,54). This relative specificity of RA target tissues was historically the first indication that the multiple functions of R, may in fact, be satisfied by different forms of the vitamin (49,52). The possibility--that RA and R may be metabolized, by their target tissues, to a common and more biologically active form--remains an ongoing area of investigation (52,54,55)..

RA metabolism into biologically inactive, excretable end products has been demonstrated in vitro using organ cultures of vitamin A deprived rat liver and testis, and hamster trachea, intestine and testis (54,55,56). In vivo, vitamin A deficient rats, after intravenous administration of RA, show accumulations of similar RA metabolites in

liver, kidney, blood, intestine and skin (52). In hamsters pre-treated with RA, the initial rates of RA metabolism, in the intestinal mucosa, were increased eight fold over that observed in vitamin A deficient animals (57). Clearly, the metabolism of RA to excretable end products does occur rapidly, both in vivo and in vitro, and is dependant upon: the tissue type, the vitamin A status of the animal, and the initial concentraion of RA to which the tissue is exposed (52,54,55,56,57).

Retinol is the predominate circulating form of vitamin A and is carried from the liver to it's target tissues by a R specific, retinol binding protein (RBP), pre-albumin complex (58,59,60). RA, in relatively small concentrations, is transported in association with serum albumin in a manner similar to long chain fatty acids (61). The cells of many target tissues, and some epithelial cancers, possess plasma membrane receptors specific for circulating R-RBP, as well as intra cellular binding proteins specific for both R (cellular R binding proteins (cRBP)) and RA (cellular RA binding proteins (cRABP)) (60,62).

Epidermal cells in particular, possess plasma membrane receptors specific for RBP (58), in addition to distinct intra-cellular R and RA binding proteins (60,62). The brief interaction of R-RBP and it's membrane receptor leaves the R molecule in an intra-cellular location while the RBP and pre-albumin are released extra-cellularily (58,60). This protein facilitated membrane transfer mechanism and

subsequent interaction with cytoplasmic carrier proteins (cRBP, cRABP) may modulate physiological stimulation by the circulating form of R or, similarly, it's primary metabolite, RA. Free RA or R (not bound to RBP, or albumin) bypasses the membrane receptor mechanism (58) and thus may influence sub-cellular events more directly, possibly as a function of cRBP or cRABP modulation (58,60,62). The epidermal presence and activity of distinct membrane and cytoplasmic R, RA receptors suggests a hormone-like action, similar to that described for the corticosteroids (63).

In epithelial target tissues, R and RA are also involved in cytoplasmic glycosyl transferase reactions leading to the synthesis of cell surface glycoproteins (64,65,66,67). Intra-cellular R and RA are phosphorylated to retinyl-phosphate (RP), which reacts with guanosine diphosphate mannose (GDP-mannose) to form mannosyl-retinyl-phosphate (MRP) and guanosine diphosphate (GDP) (64,65,66,67). This biochemical pathway parallels the glycosyl transfer reactions involving dolichol-P as a carrier of mannose in the glycosylation of membrane glycoproteins (68). Although similar, dolichol-P cannot substitute for RP in the synthesis of certain specific complex carbohydrates (64). It seems certain that the synthesis of specific glycoprotein moieties is stimulated by R and RA via retinyl-P and mannosyl-retinyl-P.

The subcellular location of glycosyl transferase reactions is not well defined but may predominate in the

smooth endoplasmic reticulum, Golgi apparatus (65,69), or alternatively, in the RER (65).

RA induced changes in the glycosylation of plasma membrane glycoproteins would suggest the possibility of secondary changes in one or more glycoprotein facilitated biological functions (64,65). RA modification of epithelial differentiation may be at least partially related to such cell surface changes.

In vitro studies concerning the effects of RA upon epithelial cell and tissue culture models have provided much enlightening data.

Cultured embryonic chick skin, in the presence of excess R, transforms from a keratinizing epithelium to a mucous secreting epithelium within 8-10 days (70,71). In the same system (72), at 2-3 days, ^{35}S uptake and secretion of glucosaminoglycans was stimulated by excess R; explants grown in control media showed relatively minimal uptake. This compares favourably with normal mucous membrane synthetic activity.

Epidermal cell cultures and skin explants of adult mammalian tissue, in comparison have also shown changes as a function of vitamin A deprivation or excess (50,73,74,75). Epidermal cell suspensions, cultured in the presence of RA excess, experience a large initial increase in DNA synthesis

and improved adherence to the substratum (49,74,75). In organ culture, explants of tracheal epithelium undergo keratinizing squamous metaplasia in the absence of RA, and then, revert back to normal, ciliated, mucous secreting epithelium when RA is added to the medium (54). Similarly, tissue explants of guinea pig ear epidermis showed marked, RA induced, secretory metaplasia; markers of keratinization (desmosomes, tonofilaments, and keratohyalin granules) were reduced and secretory elements (Golgi apparatus and secretory vesicles) were more numerous.

In addition, many in vivo studies have used adult mammalian systems to investigate the various changes induced by R and RA.

Cell mediated resistance to bacterial infection in mice is stimulated by intravenous administration of R (76). Contact sensitivity to molecular antigen however, is marginally reduced in patients treated with long term, topical application of RA (77). Thus, RA may influence the status of LC involvement in cutaneous cell mediated immunity.

Deprivation of vitamin A in the diet of mature rats, results in rapid squamous metaplasia in tracheal and intestinal epithelium (51). This result, confirmed by in vitro studies, and clearly illustrates the ability of

vitamin A to moderate epithelial patterns of differentiation.

Topical application of RA, in guinea pig, mouse, and man, induces many profound epidermal changes, including: increased mitotic activity, inhibition of keratinization, atypical differentiation and acanthosis (thickening of the epidermis). Increased DNA synthesis is an early observation after topical RA (77,78,79,80). Markers of keratinization--including desmosomes, tonofilaments, and keratohyalin granules--are significantly reduced (45,50,78). RA induced, atypical differentiation (parakeratinization) is also associated with increased synthesis, accumulation, and secretion of lipid and glycogen (45,50,78,81). Moreover, the resultant changes in the stratum corneum and concomittant increase in epidermal edema results in enhanced epidermal permeability (77). Irritant dermatitis has also been observed during the first 3-4 days of topical RA treatment in humans and indicates it's potentially toxic nature, even when used in moderate concentrations (77).

RA induction of simultaneous changes in epithelial regeneration and metabolism, forms the basis for it's therapeutic effectiveness in the treatment of epidermal scaling disorders, acneiform dermatoses(50) and, more recently, as a prophylactic agent in the prevention of carcinogen induced epithelial tumours (82).

In the present study, RA was topically applied to the skin on a daily basis in order to ensure sustained

concentrations of the biologically active molecule; thus circumventing rapid epidermal inactivation and excretion which might lead to a minimized, possibly undetectable expression of RA induced change. The correlative LM, TEM, and SEM evaluation, of resultant subcellular changes, seeks to expand the present body of information concerning RA generally, as an effector of multiple responses in a variety of tissues, and more specifically, as an influencing factor in the maintenance of keratinizing epithelia.

MATERIALS AND METHODS

Hairless Mice

Male hairless mice (hr/hr) from Jackson Laboratories, Bar Harbour, Maine, U.S.A., were crossed with a haired strain (C3H) producing haired F₁ progeny. Crossing F₁ females with hairless males produces F₂ progeny of which 50% are hairless. Of these, hairless males, 13-20 weeks old, have been used in the present study.

Retinoic Acid Treatment

RA (Sigma) in a propylene glycol vehicle--approximately 0.1 ml.--was topically applied, by gentle massage, to a 15 mm² area of the posterior dorsal epidermis. In all cases, RA treatment was performed in the morning. Animals were treated with 1% RA, 0.3% RA or unmedicated propylene glycol.

RA (1%) was applied daily for five time periods ranging from 1 to 8 days, specifically: 1, 3, 4, 6, and 8 days. Animals were sacrificed 24 hrs. after the final treatment. A duplicate was treated for 4 days and sacrificed after 2 weeks regeneration.

RA (0.3%) was applied daily for seven time periods ranging from 1 to 14 days, specifically: 1, 3, 4, 6, 8, 10 and 14 days. Again, animals were sacrificed 24 hrs. after the final treatment. Duplicate animals were treated for 8

and 14 days and sacrificed after 2 weeks.

Control animals were treated for 1, 7 and 14 days with unmedicated propylene glycol.

All treated epidermis was examined as:

- (i) Whole skin (TEM-OsO₄ fixation).
- (ii) EDTA-separated epidermis (TEM and SEM-OsO₄ and RR fixation).
- (iii) EDTA-separated dermis (SEM-OsO₄ fixation).

Tissue Processing

Animals were sacrificed by neck fracture. Skin was then removed from the posterior dorsum and cut into small pieces (2mm) for the TEM or large pieces (4-5 mm) for the SEM and LM; samples were processed for LM, TEM and SEM as indicated in Table 1. Tissue fixation, dehydration, clearing and embedding details are available in Appendix I.

Samples for the LM were fixed for 24 hours in Bouin's fixative at room temperature. For the SEM and TEM, samples were fixed with either Dalton's OsO₄ fixative for 2 hours at 4°C or, with a RR-OsO₄ fixative sequence (see Appendix I).

EDTA Separation

Skin samples were incubated in 20 mM Na₂-EDTA solution (Sigma) for 2 hours at 37 C. The EDTA solutions were prepared as described by Scaletta and MacCallum (33): NaCl, 6.83 g; KCl, 0.2 g; Na₂HPO₄, 1.15 g; KH₂PO₄, 0.2 g; 1% phenol red, 0.12 ml.; Na₂-EDTA, 7.44 g; made to 1 litre with

glass distilled H₂O. Na₂-EDTA was added to the buffer on the day of use. Epidermal sheets were separated from the dermis under a dissecting microscope using jewelers forceps. Newly separated epidermis was rinsed briefly in PBS (25°C) prior to fixation.

Adenosine Triphosphatase

Separated epidermis was stained for ATPase activity (see Appendix II) by transfer to: (a) 0.2 M trisimal buffer with 6.84% sucrose, pH 7.3, for 20 minutes (3 changes) at 4°C; (b) cacodylate buffered 2% formaldehyde, pH 7.3, for 20 minutes at 4°C; (c) 0.2 M trisimal buffer with 6.84% sucrose, pH 7.3, for 20 minutes (2 changes) at 4°C; (d) ATP-Pb staining solution, pH 7.3, for 15 minutes at 37°C; (e) 0.2 M trisimal buffer with 6.84% sucrose, pH 7.3, for 20 minutes (3 changes) at 4°C; (f) 1% solution of 22.3% ammonium sulphide for 20 minutes at room temperature; (g) 0.2 M trisimal buffer with 6.84% sucrose, pH 7.3, for 10 minutes at room temperature. Stained epidermal sheets were finally mounted dermal side up in warm glycerin jelly and examined in the light microscope.

Light Microscopy

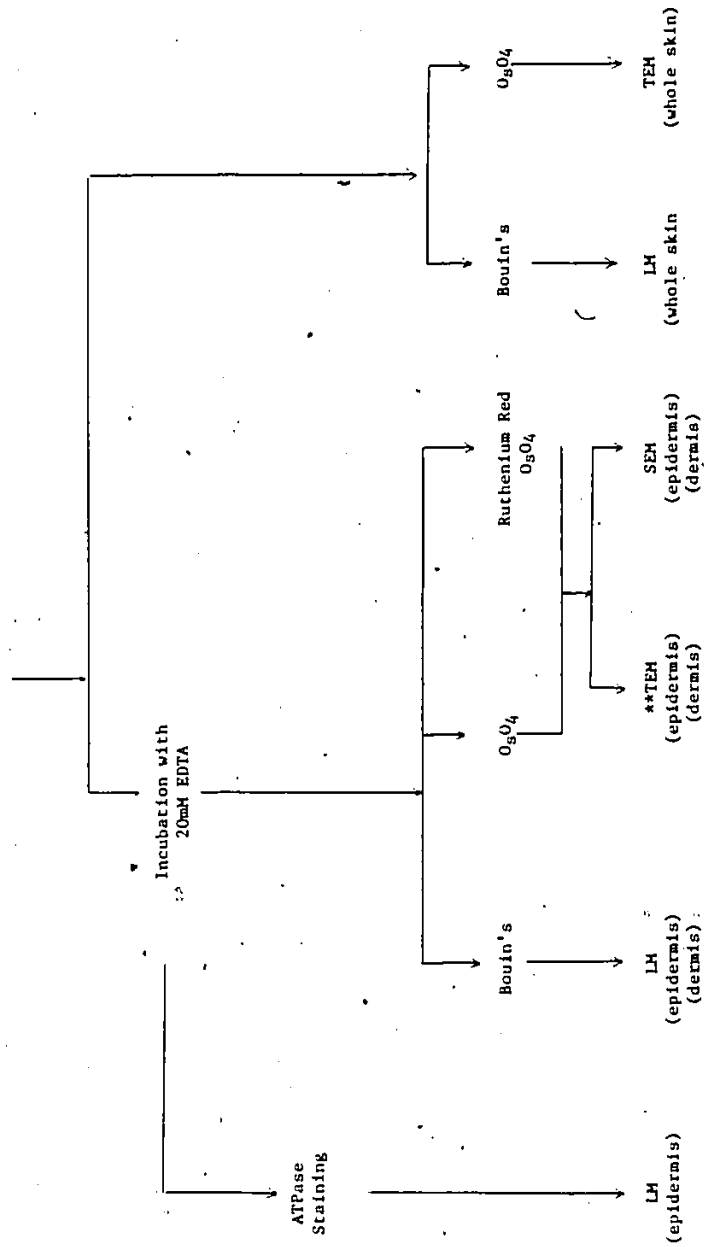
LM samples were dehydrated through graded ethanols, substituted with xylene, embedded in "paraplast" and sectioned (6µm). Sections were mounted on glass slides using egg albumin, stained with hematoxylin and eosin and then

examined and photographed in the light microscope.

Electron Microscopy

All samples, both SEM and TEM, were dehydrated through a graded series of ethanols. TEM material was substituted with propylene oxide, embedded in epon 812-araldite, thin sectioned using a Reichert ultramicrotome and, after contrasting with uranyl acetate and lead citrate, examined in either a Phillips 201 or RCA EMU-3H TEM. SEM samples were substituted with freon 13 and freon 113, critical point dried, coated with vacuum evaporated gold-palladium and examined in either an ISI-super II or a Cambridge S-180 SEM.

Table 1
Tissue Processing
Excise Whole Skin
(Normal and *Retinoic
Acid Treated)



*RA treated epidermis was not examined by LM

**whole skin - left intact after EDTA incubation - was examined by TEM after O_3O_4 fixation

RESULTS

(I) Microscopic Morphology and Organization in the Skin of the Hairless Mouse

Light Microscopy

Whole Skin

Intact epidermis (Fig. 1), stained routinely with hematoxylin and eosin (H/E), revealed numerous dermal cysts and an even array of rudimentary hair follicles. Dermal cysts variously contained keratin, lipid, and small in-grown hairs. Thin strands of epidermal tissue were often isolated in the dermis between dermal cysts and overlying hair follicles. Rudimentary hair follicles possessed active sebaceous glands and often showed an internal build-up of fatty secretions and keratinized elements. LCs were not easily discernable.

EDTA-separated Epidermis and Dermis

After EDTA incubation, the dermis was easily separated from the epidermis and showed no apparent structural damage (Figs. 2a,b). Only two epidermally derived structures remained in the dermis after EDTA separation (Fig. 2a): (i)

The dermal cysts, which were previously lacking any continuity with the external epidermis. (ii) Thin vertical strands of adnexal epidermal cells associated with the base of hair follicle pits.

The corresponding EDTA separated epidermis retained a high level of structural integrity (Fig. 2b); follicles, sebaceous glands and interfollicular epidermis were available as a unit structure. The rudimentary hair follicles were easily discerned, evenly distributed, angled away from perpendicular, and terminated with an attached pair of sebaceous glands. The products of keratinization and sebaceous gland activity were present as internal accumulations within the neck of hair follicles. Small round cells, with a relatively clear cytoplasm, were regularly distributed in positions between and below basal keratinocytes.

ATPase staining of LCs (in epidermal sheets) was frequently unsuccessful in many of the samples examined. In addition, those samples showing the expected LC distribution and morphology were often variable within a single sheet; some areas revealed very intense staining and an even LC distribution while adjacent areas showed either an absence of LCs, or diminished quantities. The effectiveness of the ATPase reaction in all samples was confirmed by the positive staining of surrounding keratinocytes. Thus, descriptions of LC distribution and morphology refer to those areas with well stained LC populations, rather than those areas with an

artifactual absence of LCs.

Epidermal sheets possessed an evenly distributed network of ATPase positive dendritic cells (figs. 3a,b). The vast majority appeared in a basal location and expressed numerous dendritic processes (3-9 dendrites). Surrounding keratinocytes showed only limited ATPase activity and thus allowed the very clear visualization of LC morphology and distribution.

Transmission Electron Microscopy

Whole Skin

Intact epidermis, contrasted with uranyl acetate and lead citrate, served to illustrate the normal organizational relationships of basal keratinocytes, LCs, and the supporting basal lamina and dermis (figs. 4a,b,c).

LCs were never observed in direct contact with the basal lamina, though they were often found in close proximity, separated only by thin underlying keratinocyte processes. LCs were of two varieties: the indeterminate cell with no cytoplasmic Langerhans granules, and the classic LC, distinguished on the basis of visible cytoplasmic Langerhans granules. Both were observed in close apposition to surrounding keratinocytes and clearly lacked any desmosomal membrane associations. They were devoid of tonofilaments,

often exhibited indented nuclei, and possessed variable compliments of lysosomes, 70-80 Å filaments, and cytoplasmic vacuoles of varied shape and dimension. Furthermore LCs often possessed abundant cytoplasmic Langerhans granules; the occurrence of LCs lacking such granules was relatively infrequent.

Basal keratinocytes were firmly adherent to the entire inter-follicular basal lamina by means of basal membrane hemidesmosome attachment sites. The basal lamina demonstrated regular contours and showed no evidence of any breaks in continuity. Pinocytotic vesicles were apparent in the cytoplasm of basal keratinocytes, usually close to or continuous with the basally oriented membrane surface.

EDTA-separated Epidermis and Dermis

Epidermis, incubated with 20 mM EDTA for 2 hours at 37°C, was examined without mechanical separation in order to discriminate between EDTA effects and those of mechanical separation using forceps (Fig. 5).

After EDTA incubation, the epidermis and dermis were often separated just above the basal lamina. Disruptions of basal cell inferior membrane surfaces were evident, as were numerous villous projections between detached hemidesmosomes. In these same areas, hemidesmosomes were often engulfed in intra-cellular vacuoles and appeared to have drawn towards the nucleus. Some cell blebbing was also evident amongst basal keratinocytes and appeared to be

associated with hemidesmosome detachment and withdrawal into the cell. Blebbing was not observed in the upper levels of the epidermis. Cell blebs possessed many free ribosomes and seemed to arise in areas of the cell recently devoid of cytoplasmic organelles. Lipid-like inclusions were sometimes observed in the cytoplasm of basal keratinocytes.

All layers of the epidermis above the basal layer were normal in their structural appearance and were unaffected by EDTA incubation.

The epidermal sheet, after EDTA incubation and mechanical separation, remained ultrastructurally intact and revealed few membranous or cytoplasmic irregularities (Figs. 6;7a,b). Desmosomes throughout the epidermis were unaffected by EDTA separation, and tight lateral associations between adjacent keratinocytes were well maintained. Basal cells however, often expressed a greater overall density than did overlying spinous and granular cells. They also showed some cytoplasmic vacuole formation (hemidesmosomes often included), an absence of hemidesmosomes, and the development of short microvillous projections of the remaining basally oriented plasma membrane.

Basal keratinocytes were partially shrunk with the normal continuum of basal epidermal cells being disrupted at regular intervals by the extrusion of intra-epidermal LCs (Figs. 6;7a;8a,b;9a,b). Basal cell processes were often

underlying partially extruded LCs in a manner closely approximating that observed in whole, unseparated control preparations (Fig. 9a). They were usually observed in close proximity to the intercellular spaces between basal keratinocytes (Figs. 8a,b;9a,b), retained their intra-epidermal processes and often interdigitated with adjacent keratinocyte membranes. LC bodies protruded downward from the overlying epidermis and possessed a highly ruffled inferior membrane surface (Figs. 8;9;10;11). LCs were also sometimes observed in pairs, usually with one cell positioned just above the other (Figs. 10;11;16a).

Ruthenium Red preparations were not as useful in the observation of intracellular ultrastructure due to the very dense staining reaction with lead citrate and uranyl acetate (Fig. 7a). However, the exposed inferior membrane surfaces of both basal keratinocytes and LCs, in uncontrasted tissue, possessed a fuzzy, well stained cell coat. Cell surfaces in the upper levels of the epidermis were poorly stained, presumably as a function of limited RR penetration through the intercellular space (Fig. 7b). Basal cells showed no intracellular staining with RR.

The dermis, after separation, possessed a basal lamina with many folds and depressions (Figs. 10b;17a,b). The folding was well illustrated by the frequent observation of a second basal lamina immediately beneath the first. This same folding sometimes accounted for some thickness variability along the length of the basal lamina as it

directly affected local sectioning angles. RR fixed dermis was well stained and possessed an overlying fuzzy coat not previously observed in tissue fixed primarily with OsO₄ (Fig. 10c).

Scanning Electron Microscopy

EDTA-separated Epidermis and Dermis

Two internal surfaces were examined by SEM after EDTA separation, the basal lamina after removal of the overlying epidermis, and the corresponding epidermal undersurface.

Preliminary SEM studies of EDTA separated epidermis have utilized standard fixation, dehydration, and clearing techniques. As such, all samples were immersed in solution and frequently agitated with no attempt at reducing physical damage or maintaining undersurface orientation for SEM observation; thus, because of curling, only small portions of the basal epidermis were available for study (Figs. 11a,b). Moreover, sub-cellular structures were markedly damaged as compared with subsequent samples processed using relatively gentle agitation during fixation.

The majority of hair follicles were broken at their base revealing intra-follicular rings of fully differentiated keratinocytes; these structures were very prominent because of their tendency to become heavily charged under the electron beam. Those few remaining intact

were striking in the absence of terminal sebaceous glands and in the ease with which the subcellular nature of the external root sheath could be examined. The majority of sheath cells were intact and frequently revealed nuclear profiles in the form of gentle surface bulges. Other cells, in contrast, appeared to have ruptured and released their contents during preparation.

The interfollicular epidermis was also much disrupted and exhibited portions of supra-basal cell layers (basal, spinous, and granular keratinocytes). The identity of exposed cell layers however, was unconfirmed in the absence of correlative TEM examination.

The dermis (Figs. 12a, b) in these initial studies was undamaged and more easily observed than samples processed using more refined preparatory techniques (Fig. 10a), as the basal lamina was relatively unobscured by overlying debris.

Because microscopic damage resulted from standard fixation, clearing and dehydration, all subsequent samples were prepared using very gentle, less disruptive handling techniques. The epidermal undersurface, after preparation with minimal agitation, provided a much improved perspective on the organization of cellular and subcellular structures (Fig. 13b).

Rudimentary hair follicles were abundant; each follicle terminated with an attached pair of sebaceous glands and was angled away from perpendicular. The external root sheath of the follicle was somewhat obscured, as compared with

interfollicular epidermis, and as such did not reveal any clear association of dendritic cells. All hair follicles were uniform in dimension and structure, with the exception of those mechanically disrupted during preparation (sebaceous glands detached, follicles broken off).

Basal keratinocytes were usually in close apposition to one another and formed a tight syncitium (Figs. 14a,b;15a,b;16b). Intercellular spaces were sometimes evident and frequently appeared close to distended LCs. The inferior plasma membrane of basal keratinocytes expressed an even distribution of microvillous projections.

LCs were widely distributed throughout the interfollicular epidermis and were easily distinguished on the basis of orientation, degree of contrast, their generally round appearance and relatively small size. More specifically, these cells possessed numerous ruffled extensions of the exposed plasma membrane surface while regions of the membrane in closer contact with surrounding keratinocytes were extended outwards in the form of slender processes (Figs. 15a,b).

Structures observed in RR preparations were essentially similar to the previous description of OsO₄ complexed material (Figs. 14b;15a;16b). However, RR fixed epidermal sheets showed a fuzzy cell coat on both keratinocytes and LCs. Blebs of amorphous material were also observed in both OsO₄ and RR preparations. These small globular structures were present close to and partially within the intercellular

5

space; thus, they correspond closely in shape and appearance to the membrane vesicles seen in the TEM.

The dermis (Figs. 10a;13a), after gentle OsO₄ fixation, displayed an overlying continuous and undisrupted basal lamina sheet. The basal lamina was often folded and possessed a variety of bulges and depressions. On occasion the basal lamina was partially torn away from the underlying connective tissue and revealed a dense matrix of collagen fibres (Fig. 12c).

RR fixation resulted in a generally fuzzy basal lamina surface and facilitated little in the way of specific structural observation.

(II) THE EPIDERMAL EFFECTS OF TOPICALLY APPLIED RETINOIC
ACID

Transmission Electron Microscopy

Whole Skin

RA induced changes were clearly similar for both 0.3% and 1% concentrations--the 1% RA however, produced more exaggerated subcellular changes at an earlier stage of treatment (Figs. 18-43). Generally, subcellular changes were indicative of strikingly increased rates of epidermal proliferation and a shift in normal patterns of cell differentiation.

Daily topical application of RA produced initial and prolonged responses that were clearly dose dependant. Two sequential epidermal responses were observed: initially, orthokeratinizing epidermis was displaced by an unusual parakeratinization and then, with continued RA exposure, returned in the form of an acanthotic orthokeratinizing epidermis.

The original stratum corneum was replaced by parakeratotic scale which differed from normal in a number of respects (Figs. 19b; 21a,b,c). Newly formed corneocytes were less flattened, extremely dense, occasionally retained an intact nucleus, and frequently possessed lipid-like droplets of various sizes.

Keratohyalin granules, membrane coating granules and tonofilaments, although not entirely absent, were strikingly reduced in both overall numbers and, in individual prominence (Figs. 18b,c,d;19a,b). Keratohyalin granules were reduced in size, lacked tonofilament association and appeared round rather than irregular. Desmosomes also, were marginally reduced in number and were often observed in a terminal location on microvillous projections of the keratinocyte plasma membrane (Figs.22a,b,c,d); they were much reduced in size and prominence, lacked normal associations with intracellular tonofilaments and were often disrupted. Hemidesmosomes were similarly lacking tonofilament support.

Concomitant with a reduction in keratinizing markers was a variety of unusual changes in the nature of epidermal cell differentiation. The nucleolus in the majority of cells was very prominent as were the corresponding synthetic structures of the keratinocyte cytoplasm. Ribosomes appeared plentiful after RA exposure, often closely associated with RER (Figs.24a,b,c). Both rough and smooth endoplasmic reticulum were strikingly prevalent in all epidermal cell layers.

The Golgi apparatus was also generally increased, especially in the uppermost cell layers where it was unusually abundant (Fig. 24a). Golgi vesicles and RER were often positioned close to newly formed lipid droplets; these were present in all layers of the epidermis though most

plentiful in the uppermost cell layers (Figs.24c;28), including the newly formed parakeratotic scale (Figs. 21a,c,d).

A sparse distribution of lipid droplets was first observed after 3 days exposure to both 0.3% and 1% RA. After 6 days exposure to 1% RA, and 8 days exposure to 0.3% RA, droplets were abundant in all layers of the epidermis. Epidermis treated daily with 1% RA showed initial lipid synthesis by 2-3 days, maximum synthesis at 5-6 days and a reduction in lipid synthesis by 8 days. Epidermis exposed to 0.3% RA concentrations began to show signs of lipid synthesis after 2-3days, reached a maximum at 7-8 days and decreased to a total absence of lipid synthesis by 10 and 14 days. Animals treated with RA and allowed 2 weeks epidermal regeneration were lacking any evidence of lipid synthesis (Figs.20a,b).

Glycogen was sparsely distributed in the cytoplasm of basal and spinous cells after 3 daily applications of 1% RA and after 5 daily applications of 0.3% RA; it was present in all subsequent time periods treated with 1% RA and up to 8 days post treatment with 0.3% RA. The distribution of glycogen was sparse in all samples and, when concentrated, was located in a perinuclear position (Fig.24b).

The intercellular space was significantly enlarged by 3 daily applications of either 0.3% or 1% RA (Figs. 22a,b,c,d); again the effects of the 1% RA were more pronounced than those of 0.3% RA. Spaces between basal and

spinous cells, and to a lesser extent amongst the cells of the granular layer, were most prominent after 5 and 3 days exposure to 0.3% and 1% RA respectively. Spaces were still marginally enlarged after 8 daily applications of 1% and 0.3% RA. However, after 10 days of 0.3% RA, spaces were reduced to normal dimensions.

The plasma membranes of basal and spinous cells were irregular, occasionally disrupted and possessed numerous short processes penetrating into the intercellular space. Desmosomes often occupied a terminal position on such microvillous membrane extensions, were diminished in number and lacked reinforcement from intracellular tonofilaments. They retained cell to cell contact but, were often under apparent stress due to increasing intercellular fluid pressure.

In epidermis treated for 3 and 6 days with 1% RA, an accumulation of poorly contrasted granular material was observed within the intercellular space, often in close association with cell degeneration (Figs. 22b,d;25). The basal lamina assumed an irregular profile shortly after initial RA exposure and retained this profile in all RA treated epidermal samples.

In some samples, after 3 and 6 daily applications of 1% RA, the irritant nature of RA was evidenced by abundant epidermal infiltration of histiocytic elements (monocytes, polymorphonuclear leukocytes) leading to the formation and sloughing of high level intra-epidermal micro-abscesses

(Figs. 26a,b; 27a,b; 44a,b). The underlying dermo-epidermal junction was frequently disrupted by histiocytes as they migrated across the basal lamina and into the epidermis (Fig. 27a,b).

Intra-mitochondrial inclusions (IMI) were frequently present in all layers of the epidermis after treatment with either 0.3% or 1% RA (Figs. 23c; 24b,c; 28); these inclusions were observed in many stages of development within a single epidermal sample. They appeared to begin initially as a small, moderate electron-dense sphere within the mitochondrial cristae, undergo enlargement and then physically disrupt the inner mitochondrial membranes. The "mature" IMI was found within damaged mitochondria, partially within ruptured mitochondria or free in the cytoplasm.

Epidermis treated by prolonged daily applications of 1% and 0.3% RA was generally normal in its appearance 14 days after termination of RA treatment. However, the sample treated with 0.3% RA for 14 days remained marginally thickened by an increased number of cell layers in the stratum corneum.

LCs appeared normal up to 72 hours after the beginning of daily 0.3% and 1% RA application. At 3 days exposure, LCs were infrequently observed after 1% RA and, after 0.3% RA, often appeared in pairs. When observed, LCs were usually in a supra-basal rather than basal location and were metabolically active, showing prominent Golgi, RER, and

lysosomes.

Intimate associations of epidermal LCs and incoming histiocytes was not observed. LCs did not appear to be sloughed off with external parakeratotic scale. After prolonged exposure (10 and 14 days) to 0.3% RA, LCs were normal in location and structure.

EDTA-separated Epidermis--OsO4 Fixation

EDTA separated samples were particularly effective in highlighting and expanding upon previous observations derived from RA treated whole skin samples. Lipid synthesis, hemidesmosome structure, desmosome character, the general metabolic state of the epidermal cell cytoplasm and the extracellular release of cytoplasmic elements was more easily perceived. Most significantly, TEM observations, of structures present at the dermo-epidermal interface, complement SEM observation of the same or similar structures; thus allowing a more enlightened interpretation of change.

Hemidesmosomes, in contrast with those in normal epidermis, were abundant. The majority retained their normal position on the basal cell plasma membrane and only a limited number were observed within cytoplasmic vacuoles (Figs. 31a; 32a,b,c,d; 41a,b,c). They also lacked normal associations with tonofilament aggregates.

The cells of the lower stratum spinosum (and occasional basal cells) were uniformly electron dense after uranyl

acetate and lead citrate staining, as compared with the fine contrast of overlying cells and the majority of basal cells (Figs. 29; 30a,b,c).

The development of intercellular spaces was accentuated in separated epidermal preparations (Figs. 29; 30a,b,c; 31c). As observed in whole skin preparations, they were most predominate during the early stages of RA treatment (3-5 days) and, after 6 days exposure were clearly diminished.

Lipid droplets were observed in all layers after RA exposure (Figs. 29; 31b). The complex of RER, Golgi, free ribosomes and newly produced lipid droplet were delicately preserved and contrasted; thus providing an improved view of RA induced intracellular lipid synthesis.

Membrane bound blebs of cytoplasm were frequently observed in continuity with, and in close proximity to, the ventral surface of basal keratinocytes (Figs. 32a,b,c,d; 33a,b; 29a); and to a lesser extent amongst the cells of the spinous layer. They were most often in close association with areas of the basal keratinocyte membrane previously occupied by hemidesmosomes; though they possessed no hemidesmosomes on their surface. The overlying cytoplasm frequently revealed a peri-nuclear condensation of organelles, including newly phagocytized hemidesmosomes. Two varieties of cell bleb were observed: (1) Membrane enclosed cytoplasm containing few vacuoles and numerous ribosomes (Figs. 32a,b; 33b). (2) A membrane enclosed structure containing one to many vacuoles, each surrounded by a thin

layer of peripheral cytoplasm (Figs.31c;32c,d); vacuoles lacked an enclosing membrane and contained fibrous material. In addition, microvillous projections of the basal cell plasma membrane, sometimes in continuity with externalized blebs, often contained enclosed vacuoles (32d).

EDTA-separated Epidermis--RR Fixation

Epidermal sheets, from RA treated mice, separated by Na₂-EDTA and fixed with RR as a ligand of OsO₄, were examined by TEM.

In uncontrasted sections (no uranyl acetate or lead citrate) the penetrating qualitys of RR were readily apparent (Figs.33a;36). It's intra-cellular penetration was also weakly, yet easily discernable (Figs.33a;34a,c,d). Moreover, RR clearly illustrated the glycoprotein of the cell coat (Figs. 33a;34d) and the filamentous nature of separated hemidesmosomes (Figs.34c,d). In particular, it highlighted the glycoprotein laminate structure of membrane coating granules occuring in the cells of the stratum granulosum (Fig. 36).

Contrasting of sections with uranyl acetate and lead citrate resulted in the overall enhancement of structures already contrasted with RR (Figs.33b;34b;35). Extracellular penetration and staining in the upper epidermis (str. spinosum and str. granulosum) was more abundant in tissue from RA treated animals (Figs.33b;35).

Basal cell blebs, both free and attached, were again observed in all RA treated epidermis. Basal cells (especially those with enlarged ventral cell bodies) and closely associated membrane vesicles revealed intracellular penetration and staining with RR-- often in close association with visible disruptions of the plasma membrane (Figs. 33b;34a,b,c,d).

Hemidesmosomes were never observed on the plasma membrane of the enlarged ventral cell bodies of basal keratinocytes (Figs. 33b;34b), nor were they present on the surface of free or attached membrane vesicles (Figs. 33a;34a,c,d). However, hemidesmosomes were observed on the plasma membrane of unenlarged ventral cell bodies--usually in close proximity to underlying free vesicles (Figs. 33a;34c,d)--and as aggregates within peri-nuclear vacuoles in the cytoplasm of enlarged basal keratinocytes (Figs.33b;34b). Intracellular hemidesmosomes were not stained with RR (Figs. 33b;34b); in contrast, extracellular hemidesmosomes were well stained with RR (Figs. 33a;34c,d).

RR readily penetrated the intercellular space in RA treated epidermis. After 6 daily applications of 0.3% RA, when the epidermis was undergoing a transformation from abnormal to normal patterns of differentiation, RR staining highlighted the elaborate membrane interdigitations occurring amongst the cells of the stratum spinosum and lower stratum granulosum (Figs.33b;35); the complexity of these cellular associations was not as easily apparent after

standard OsO₄ fixation.

Scanning Electron Microscopy

EDTA-separated Epidermis

RA induced a number of changes in the subcellular structure of separated epidermal sheets. Generally, all observed changes were similar in character and varied only in the degree of their intensity as determined by the duration of exposure and the concentration of RA. Cell blebbing was abundant, intercellular spaces were enlarged, hemidesmosomes were retained on the surface of basal keratinocytes and fibrous debris was often abundant.

Cell blebbing was observed in both RA treated and untreated epidermis, however, treated samples were clearly distinct in both the nature and extent of visible cell blebs. Blebs ranged from very minute to very large (3 μ m) and assumed an endless variety of globular shapes (Figs. 37;38;39;40;41). They appeared to arise either directly from the basal cell surface or, less directly from elongate projections of the cell surface (Figs. 40a,b) (both events correlate with TEM observations); many blebs were intimately associated with the intercellular space and were clearly derived from intra-epidermal keratinocytes or the less exposed, lateral portions of basal keratinocytes.

The widening of the intercellular space has allowed

observation of the lateral surfaces of basal keratinocytes and has revealed a clear difference between areas of hemidesmosomal and desmosomal adherence (Figs. 41a,b,c). Microvillous projections of the lateral cell surface correlate with TEM observations of microvilli with terminal desmosomes. Projections were sparsely distributed on an otherwise smooth surface. Some basal cells, in comparison, possessed an apparently degenerate cell surface comprised of an abundant network of web-like elaborations.

Hemidesmosomes were abundant and retained their *in vivo* orientation on the ventral surface of basal keratinocytes. At low magnification, RA treated keratinocytes appeared smooth and flat when compared with untreated keratinocytes which displayed ruffled surfaces as a function of hemidesmosome invagination. Hemidesmosomes in RA treated epidermis, having retained their external location, could be very clearly observed by SEM at higher magnifications; they were numerous and often formed linear aggregates.

LCs were not easily discernable in the majority of RA treated samples; extensive cell blebbing and debris did not allow LC identification. Only in marginally affected, near normal samples, were LCs obvious and identifiable (Figs. 37a; 42a,b,c). LCs were observed in epidermis that was normal, treated for 24 hours (1% and 0.3% RA), treated for longer than 10 days (0.3% RA) and finally, in epidermis allowed 2 weeks regeneration after the termination of RA treatment. Epidermis, after 24 hours exposure to RA, was

essentially normal in it's SEM appearance. Intercellular spaces were marginally larger, but LCs and keratinocytes remained morphologically and distributionally unaltered.

After prolonged exposure to RA (10 days), the epidermal undersurface again appeared normal in most respects. RA induced change was demonstrated only by the relative abundance of fibrous material underlying the syncytium of basal cells.

RA treated samples (8 and 14 days, 0.3% RA) allowed 14 days regeneration, possessed tighter lateral associations of basal keratinocytes and LCs were abundant, as were numerous small cell blebs resembling those observed in normal epidermis.

Control epidermis, treated topically with unmedicated propylene glycol for 7 and 14 days, was normal in it's SEM features.

EDTA-separated Dermis

The basal lamina remained intact after topical exposure to RA and after separation with EDTA. The basal lamina and it's underlying dermal matrix revealed increasingly irregular features as RA exposure time and concentration were increased (Figs. 43a,b,c; 44a,b). Folds and shallow depressions became more numerous and complex at times of maximum change, 4 and 6 days 1% RA and 6 days 0.3% RA respectively. After prolonged RA treatment (10 and 14 days),

the dermal surface returned to a relatively smooth SEM appearance. Cells and cell blebs were not observed in any of the dermal samples examined by SEM.

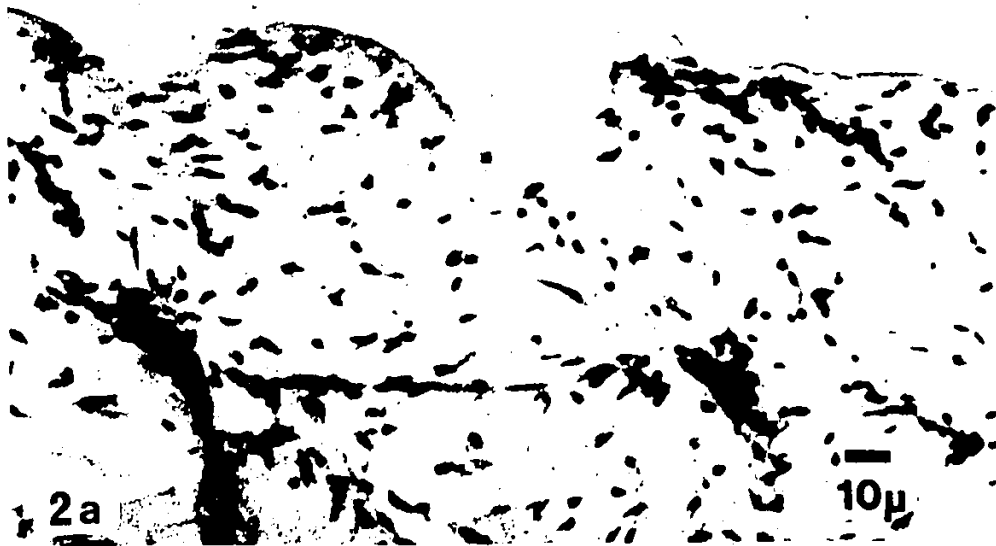
Figure 1 LM. H/E. Normal skin; dermal cysts (arrows) variously contain keratin, sebum and small hairs; strands of epithelium extend into the dermis from the point of sebaceous gland attachment to rudimentary hair follicles.

300x



Figure 2

- (a) LM. H/E. Normal, EDTA-separated epidermis; LCs (arrows) protrude downwards from the basal surface; the inter-follicular epidermis, rudimentary hair follicles and sebaceous glands are completely intact. 700x
- (b) LM. H/E. Normal, EDTA-separated dermis; the basal lamina is retained intact, as are the thin strands of dermally oriented epithelium. 700x






Figure 3 LM. ATPase staining, normal, EDTA-separated epidermis; (a) LCs are evenly distributed and easily distinguished. 300x
(b) A single LC showing the characteristic dendritic morphology. 600x



Figure 4 TEM. UA/LC. Normal skin: (a) Normal epidermis and dermis showing the association of basal lamina and basal keratinocytes, the stratum basale, stratum spinosum, stratum granulosum, and stratum corneum. Two LCs (L) are present in the basal layer. The circle and square are enlarged in Fig. 4b and 4c respectively. 5,143x

(b) Classic Langerhans granule showing continuity with the external plasma membrane. Enlarged from Fig. 4 (a). 14,400x

(c) Abundant Langerhans granules in the perinuclear cytoplasm. Enlarged from Fig. 4 (a). 14,400x

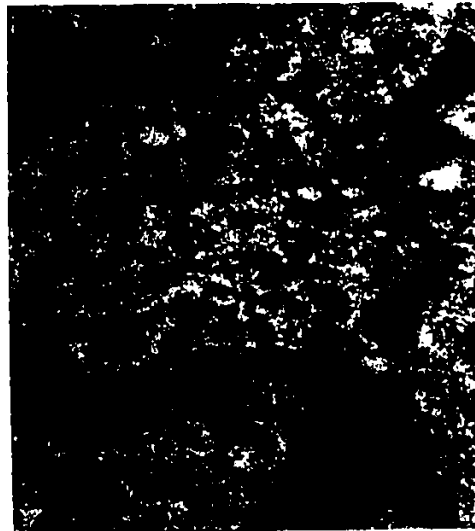


Figure 5 TEM. UA/LC. Normal skin (epidermis and dermis) incubated with EDTA but left intact. Basal keratinocytes and basal lamina have separated, hemidesmosomes (arrows) are invaginated and LCs (L) are still present in an intra-epidermal location. 43,917x



Figure 6 TEM. UA/LC. Normal, EDTA-separated epidermis;
LCs (L) are extruded from between basal keratinocytes and
ultrastructural change from EDTA separation is minimal.
5,683x



Figure 7 TEM. Normal, EDTA-separated epidermis; (a) EDTA-separated epidermis after RR fixation, critical point drying and contrasting with UA/LC. 6,616x
(b) EDTA-separated epidermis prepared as 7 (a) but left uncontrasted with UA/LC. 7,138x

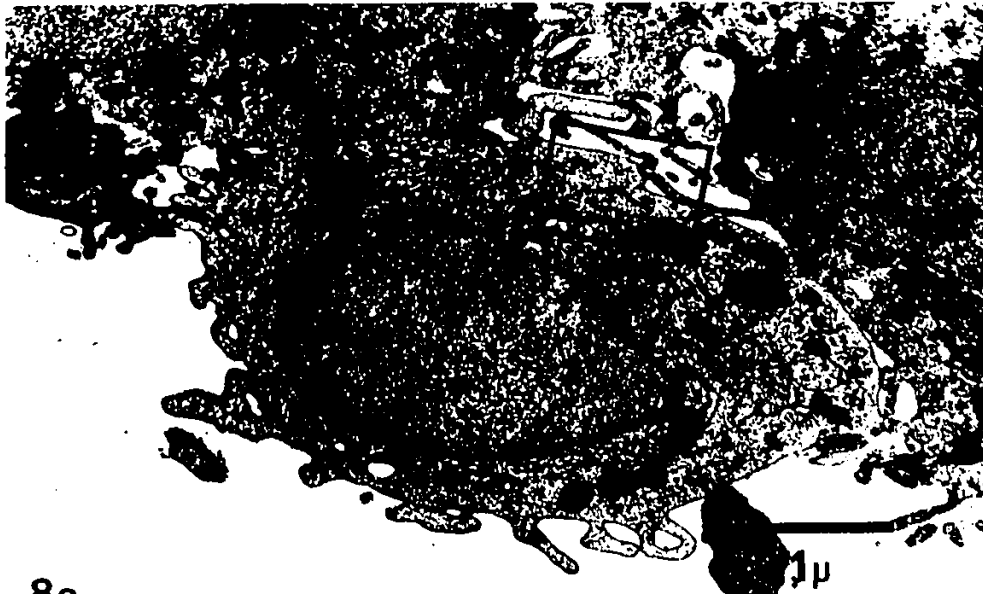


7a

Figure 8 TEM. UA/LC. Normal, EDTA-separated epidermis:

(a) LCs are extruded from between basal keratinocytes. The area delineated by the square includes a single Langerhans granule and is enlarged in Fig. 8 (b). 20,000x

(b) Langerhans granule enlarged from Fig. 8 (a). 120,000x



8a



8b

Figure 9 TEM. UA/LC. Normal, EDTA-separated epidermis:

(a) Paired LCs. 11,000x

(b) Protruding LC with underlying process of basal
keratinocyte. 11,000x

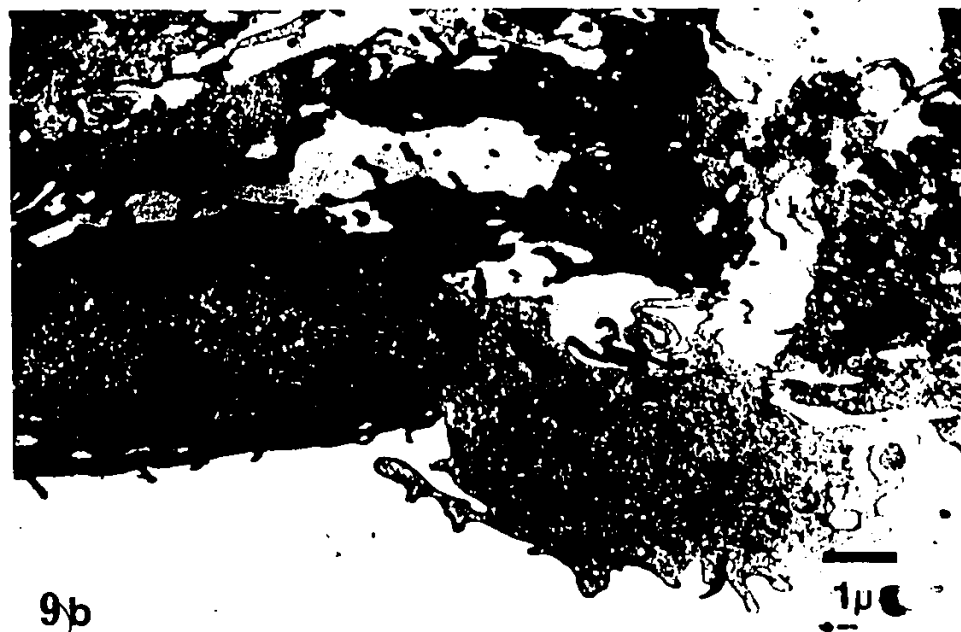


Figure 10 EDTA-separated dermis: (a) SEM. Basal lamina is intact and relatively featureless. 1,200x
(b) TEM. Basal lamina, OsO₄ fixation. 120,000x
(c) TEM. Basal lamina, RR fixation. 70,000x

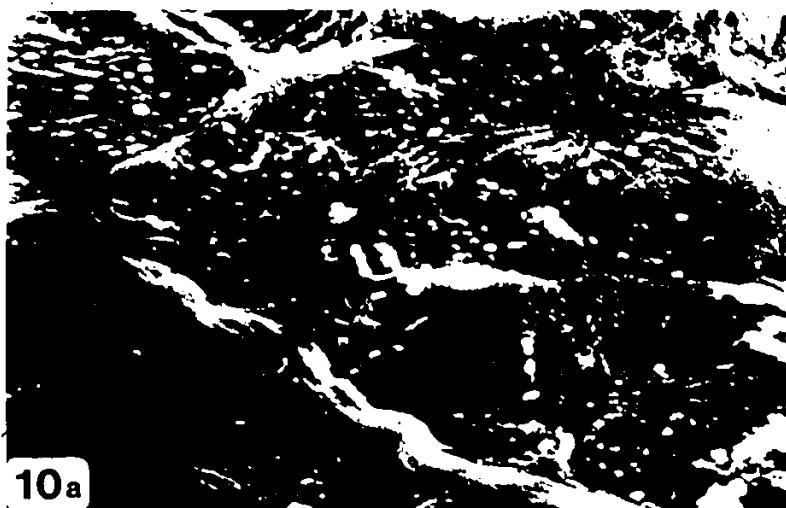


Figure 11 SEM. EDTA-separated epidermis: (a) Overview showing the loss of follicles and the damage created by the use of agitation during preparation. Area indicated by arrow enlarged in Fig. 11 (b). 109x

(b) Hair follicle enlarged from Fig. 11 (a). 1,130x

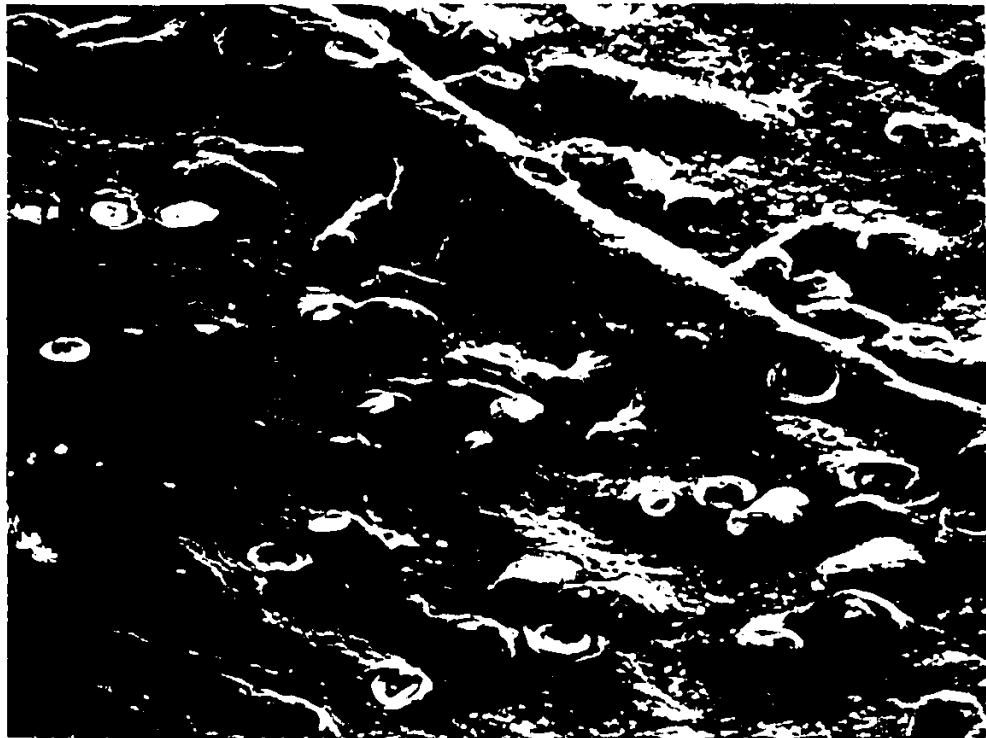


Figure 12 SEM. EDTA-separated dermis showing the relatively minor effects of agitation during preparation:

(a) Low magnification perspective, hair follicle pits are abundant and randomly distributed. 107x

(b) Inter-follicular basal lamina is smooth as compared with the walls of hair follicle pits. 749x

(c) Basal lamina (on the left) has been partially removed (right), revealing the collagen fibres of the underlying connective tissue. 315x

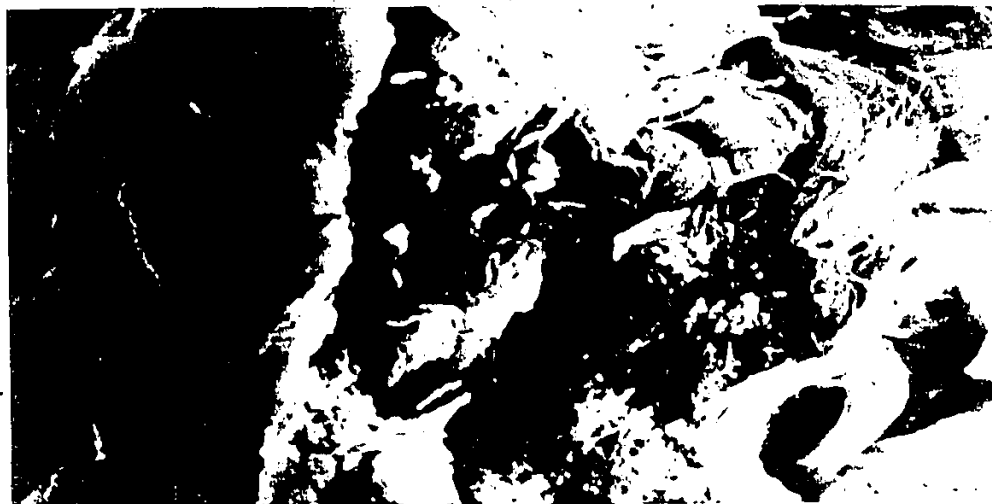
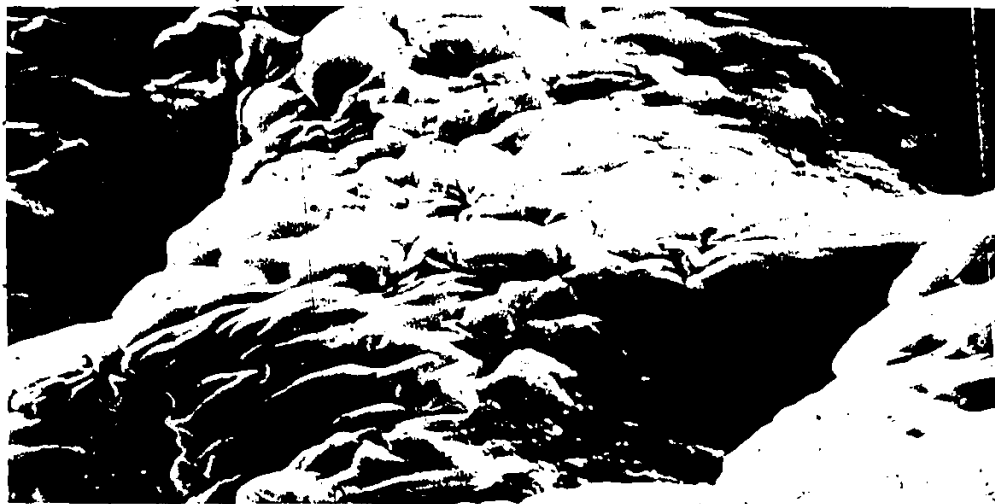
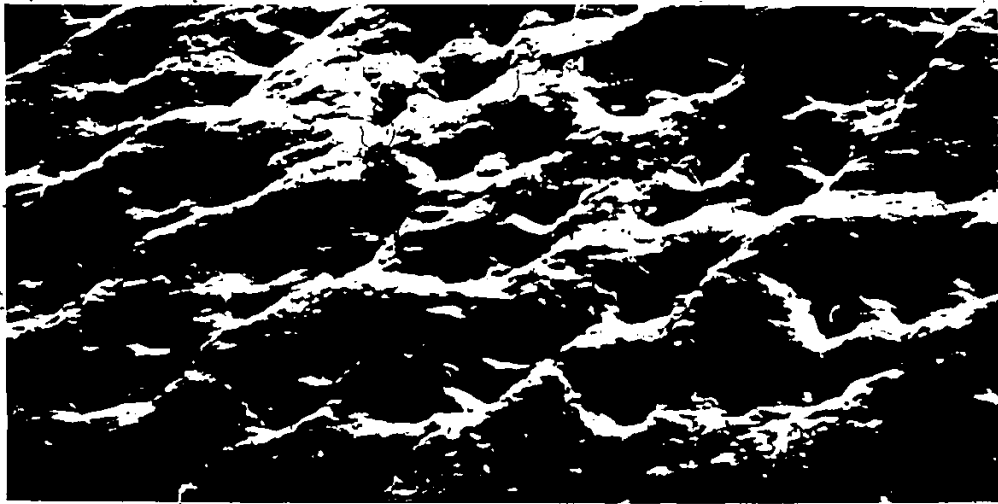


Figure 13 (a) EDTA-separated epidermis. Sebaceous glands are present in a terminal location on all hair follicles.

LCs (round, elevated and slightly charged) are evenly distributed over the basal epidermis between follicles. 250x

(b) Dermal counterpart to the preparation shown in Fig.

13(a). 300x

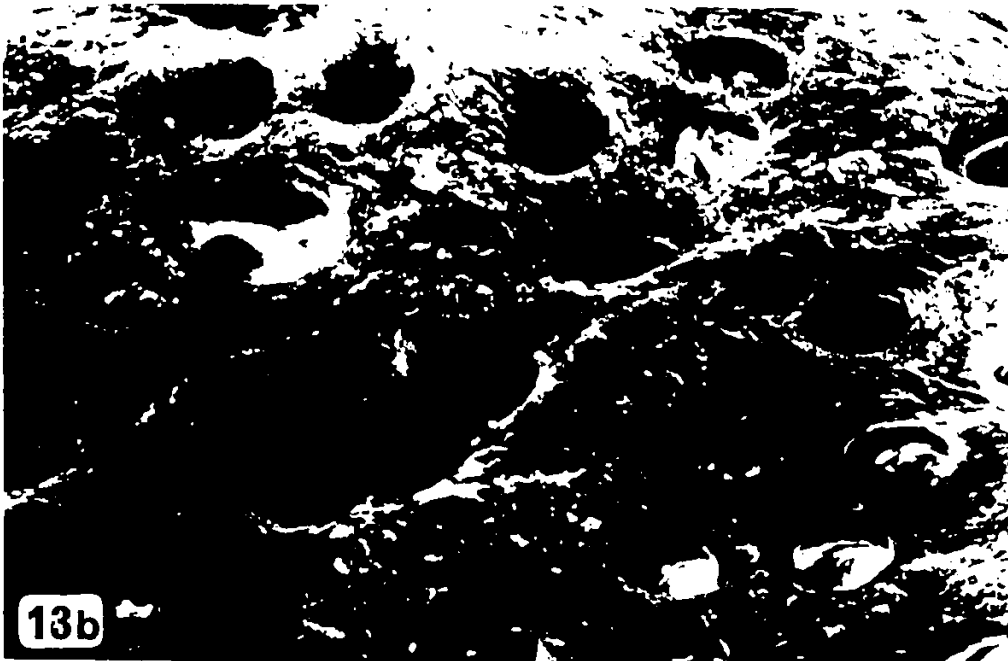




Figure 14 SEM. EDTA-separated epidermis: (a) LC (arrow) and basal keratinocytes. 2,760x
(b) Numerous LCs protruding from the basal epidermis. 1,656x

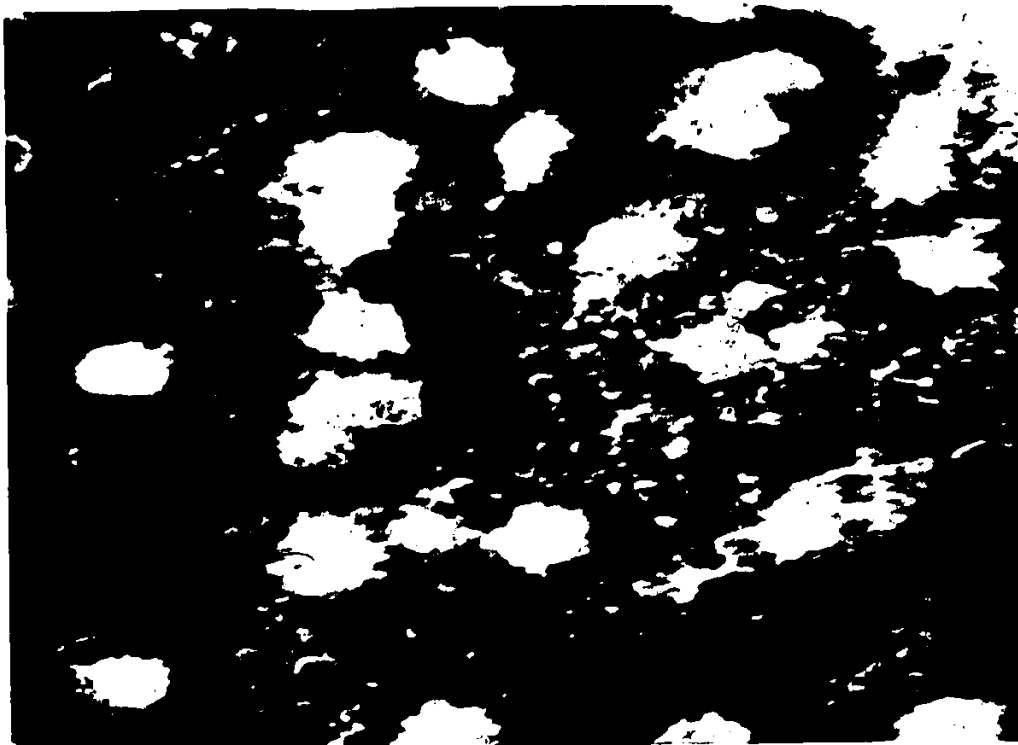
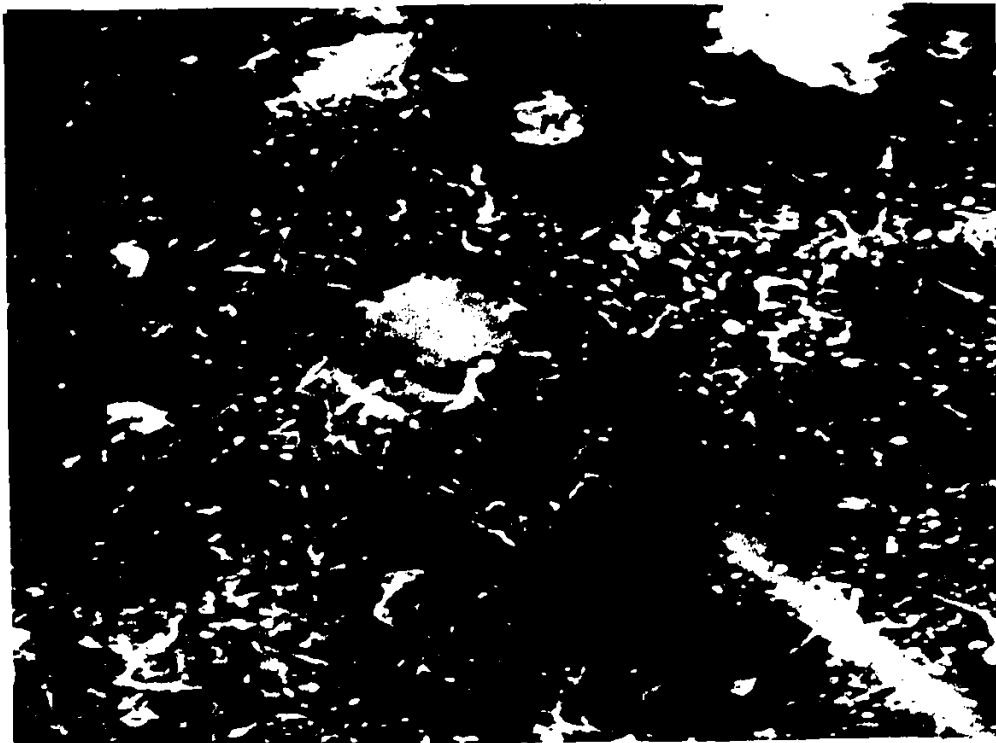


Figure 15 SEM. EDTA-separated epidermis: (a) LC (centre)
and membrane vesicle (upper right), RR fixation. 8,000x
(b) Paired LCs, OsO4 fixation. 6,000x

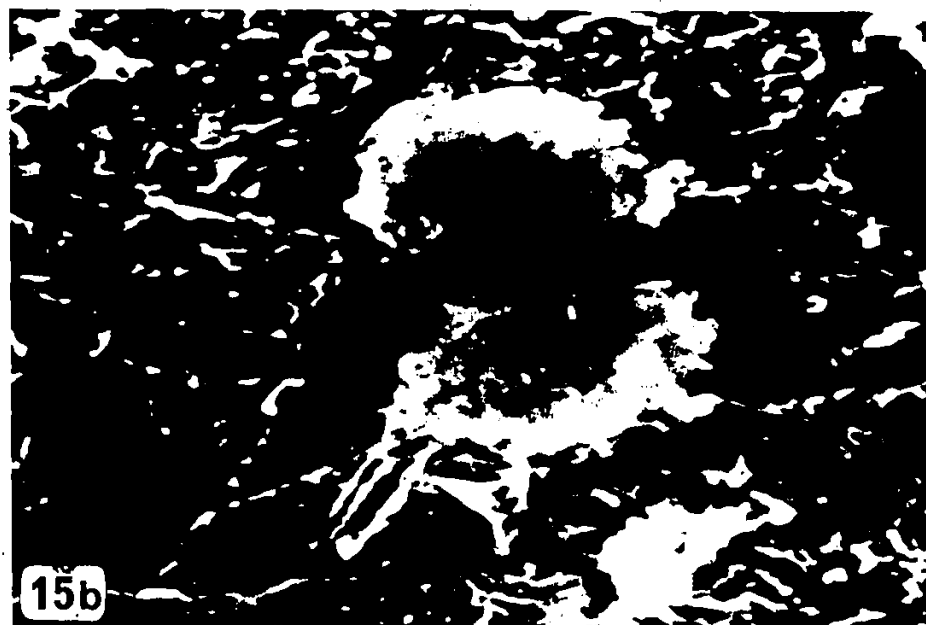
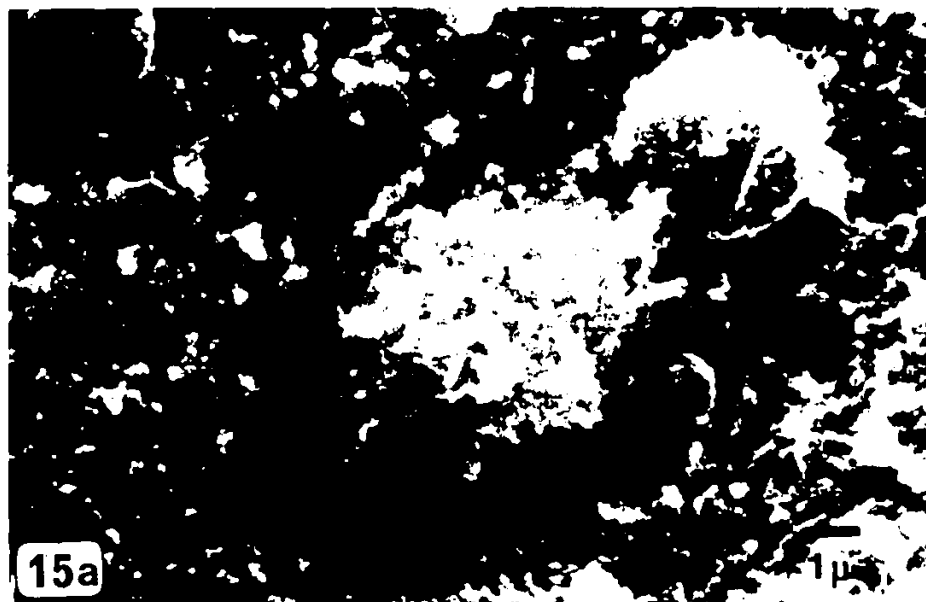


Figure 16 EDTA-separated epidermis: (a) TEM. Two LCs are subjacent to the epidermis while a third (L) remains in an internal location. 13,500x

(b) SEM. Membrane vesicles (V) and LCs (L), RR fixation. 5,000x



16a

1μ



16b

Figure 17 TEM. EDTA-separated dermis: (a) The basal lamina has remained intact after EDTA separation. 21,100x
(b) The presence of a double basal lamina confirms the folding observed in SEM preparations. 125,000x

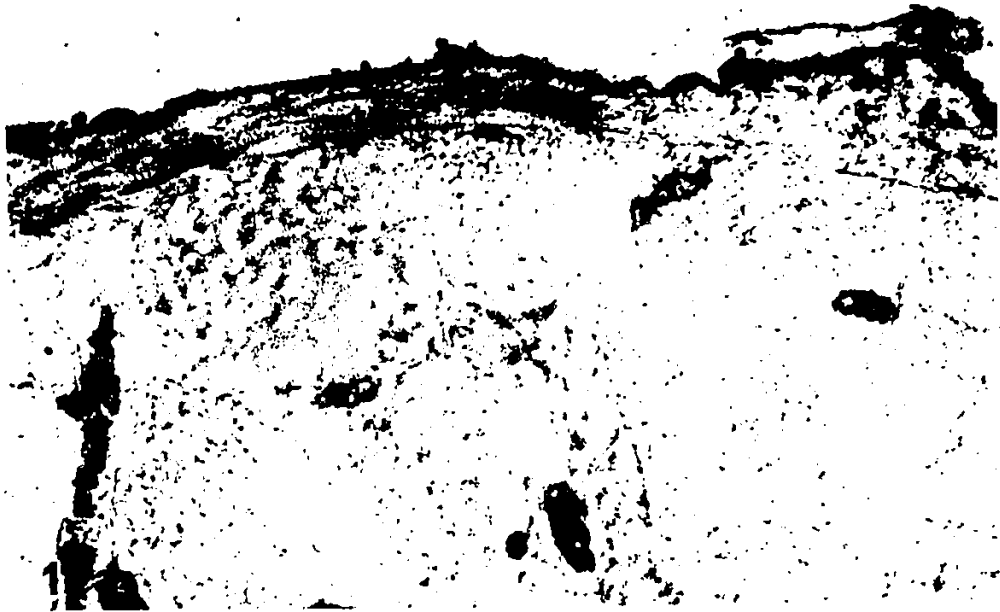


Figure 18 TEM. RA treated epidermis:

- (A) 1% RA, 24 hours. 3,657x
- (B) 0.3% RA, 3 days. The area within the box is enlarged in Fig. 22 (A). 2,628x
- (C) 0.3% RA, 5 days. 2,640x
- (D) 0.3% RA, 8 days. 2,640x

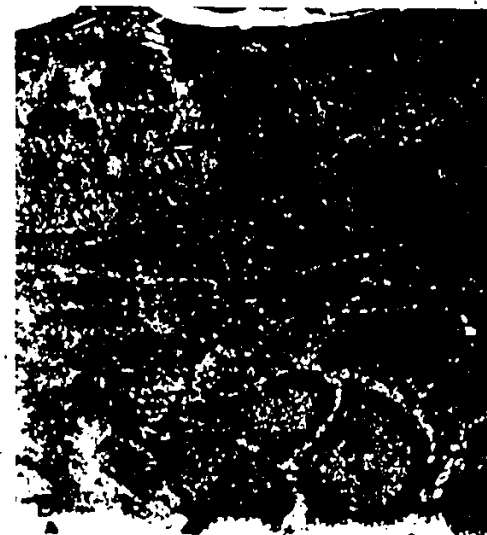


Figure 19 TEM. RA treated epidermis:

- (A) 1% RA, 3 days. 2,640x
- (B) 1% RA, 6 days. 4,392x
- (C) 0.3% RA, 10 days. 6,742x
- (D) 0.3% RA, 14 days. 5,500x

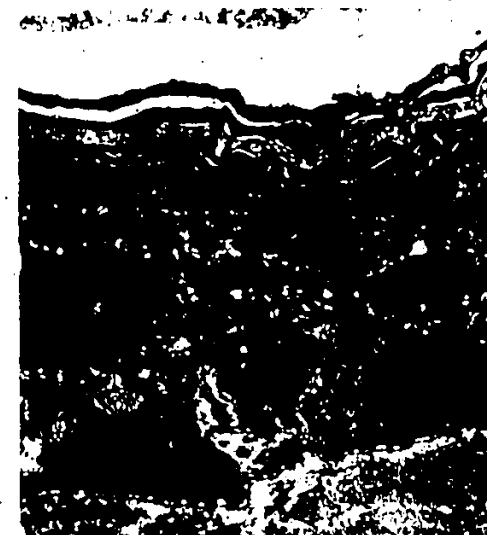


Figure 20 TEM.

- (A) Treated epidermis: 0.3% RA, 8days. 5,500x
- (B) Treated epidermis: 1% RA, 4 days. 2,750x
- (C) Control: Propylene glycol, 7 days. 2,750x
- (D) Control: Propylene glycol, 14 days. 7,913x

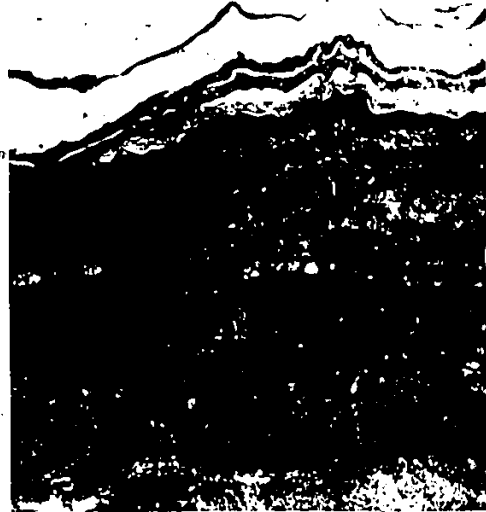
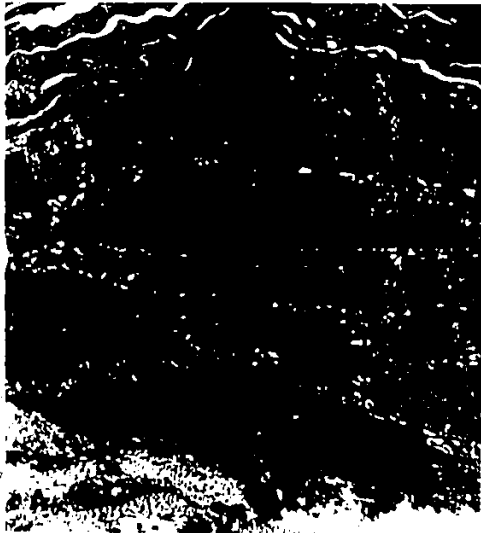


Figure 21 TEM. RA-treated epidermis:

- (A) 1% RA, 6 days. Stratum corneum and upper stratum granulosum; note the abundance of lipid-like droplets and the absence of cytoplasmic filaments, keratohyalin granules and membrane coating granules. 8,000x
- (B) 0.3% RA, 5 days. Lower stratum corneum and upper stratum granulosum; the uppermost corneocytes have been lost during processing. 5,554x
- (C) 0.3% RA, 8 days. Keratohyalin granules are returning to normal dimensions while lipid-like granules remain abundant. 5,554x
- (D) 0.3% RA, 5 days. Upper stratum corneum; corneocytes are increased in number and lipid-like droplets are abundant. 3,703x

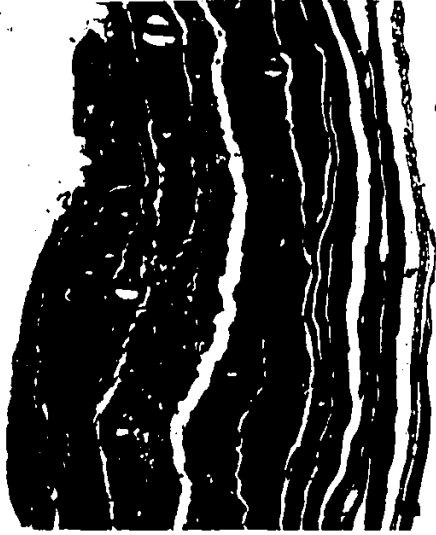


Figure 22. TEM. RA treated epidermis:

(A) 0.3% RA, 3 days. This micrograph is a higher magnification view of the area included in the box, Fig. 18b. Enlargement of the intercellular space and development of membrane elaborations amongst cells of the stratum spinosum. 16,285x

(B) 0.3% RA, 5 days. Plasma membrane elaborations with terminal desmosomes extend into the enlarged intercellular space of the stratum spinosum. Association between cells is limited to areas of desmosomal contact. Intercellular granular material is abundant. 8,925x

(C) 1% RA, 3 days. Desmosome association between keratinocytes in the stratum spinosum; note the absence of intracellular tonofilament support and the abundance of polyribosomes and endoplasmic reticulum. 33,333x

(D) 1% RA, 8 days. Membrane elaborations and granular material in the intercellular space between keratinocytes of the stratum spinosum. 11,600x

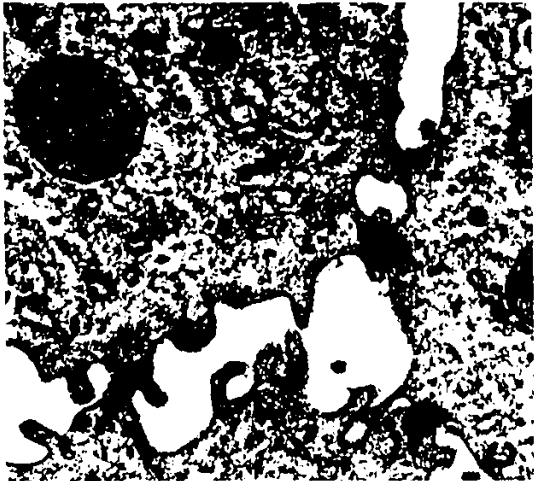
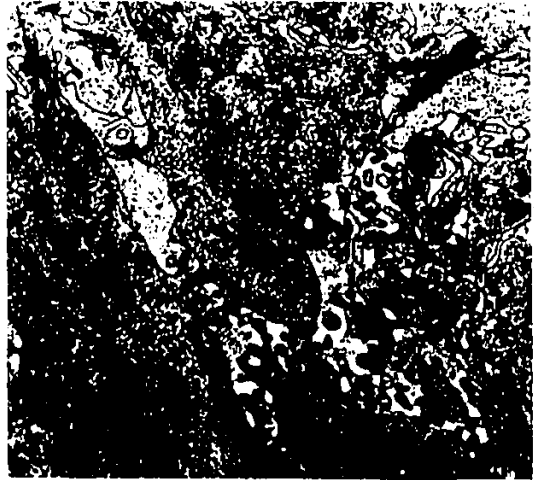
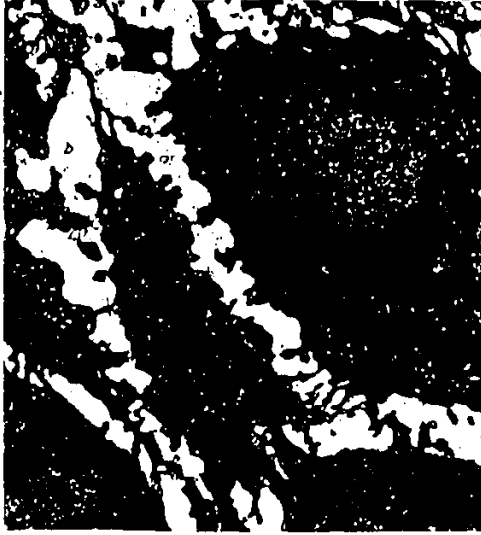


Figure 23 TEM. (a) Normal epidermis; hemidesmosomes (large arrows) associated with the basal lamina. Pinocytotic vesicles (small arrows). 82,286x

(b) 1% RA, 3 days; hemidesmosomes associated with the basal lamina. Pinocytotic vesicles are not as abundant. 66,667x

(c) 0.3% RA, 8 days; the intercellular space between hemidesmosomes is slightly enlarged. Intra-mitochondrial inclusions (I). 37,714x

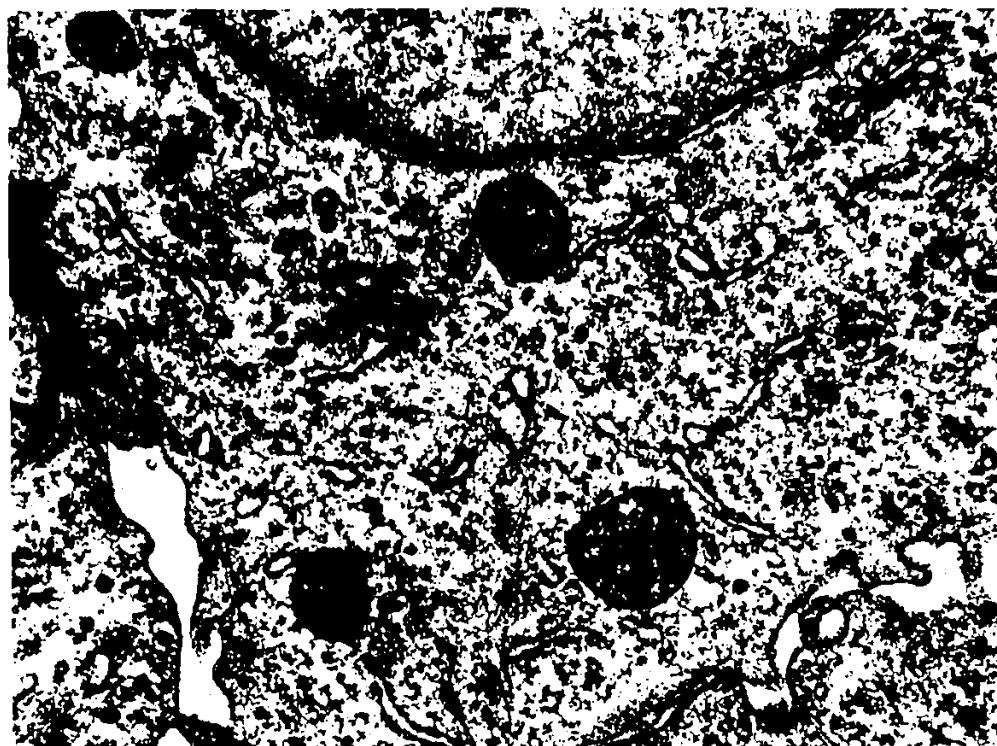
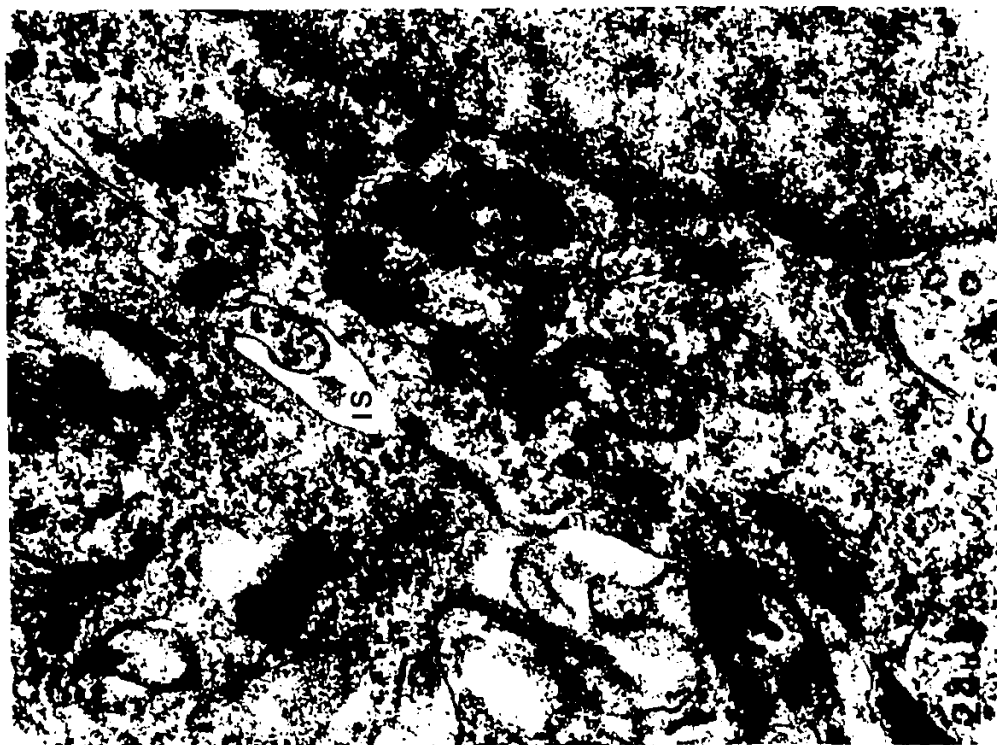


Figure 24 TEM. RA treated epidermis. Cytoplasm of spinous keratinocytes:

(a) 1% RA, 3 days. Note the absence of tonofilaments, dilated cisternae of RER, numerous polyribosomes and active perinuclear Golgi apparatus and associated vesicles (arrows). Nucleus (N). 36,833x

(b) 0.3% RA, 8 days. Glycogen (pointer) is present in a perinuclear location. A single intra-mitochondrial inclusion is present just beneath the pointer. Nucleus (N).

Intercellular space (IS). 36,571x



✓ Figure 24 (cont'd from previous page)

(c) 1% RA, 6 days. Lipid-like droplets show an irregular profile and suggest continuity with surrounding RER and, each other. Two intra-mitochondrial inclusions are present in the upper left; the larger is surrounded by an irregular membrane, possibly the remnants of mitochondrial cristae.

36,571x



Figure 25 TEM. RA treated epidermis, 0.3% RA, 5 days.
Enlarged intercellular space between basal keratinocytes
containing granular material. The underlying basal lamina is
extremely irregular in profile. 18,463x



Figure 26 TEM. RA treated epidermis, 1% RA, 3 days: (a) Polymorphonuclear leukocytes (P) migrate into the epidermal compartment, aggregate and are then sloughed along with surrounding keratinocytes. 2,743x

(b) A flattened keratinocyte underlies a tight aggregate of 4 polymorphonuclear leukocytes (P) similar to those shown in Fig. 26 (a). Two migratory leukocytes, and abundant granular debris, are present in the underlying intercellular space.

7,750x

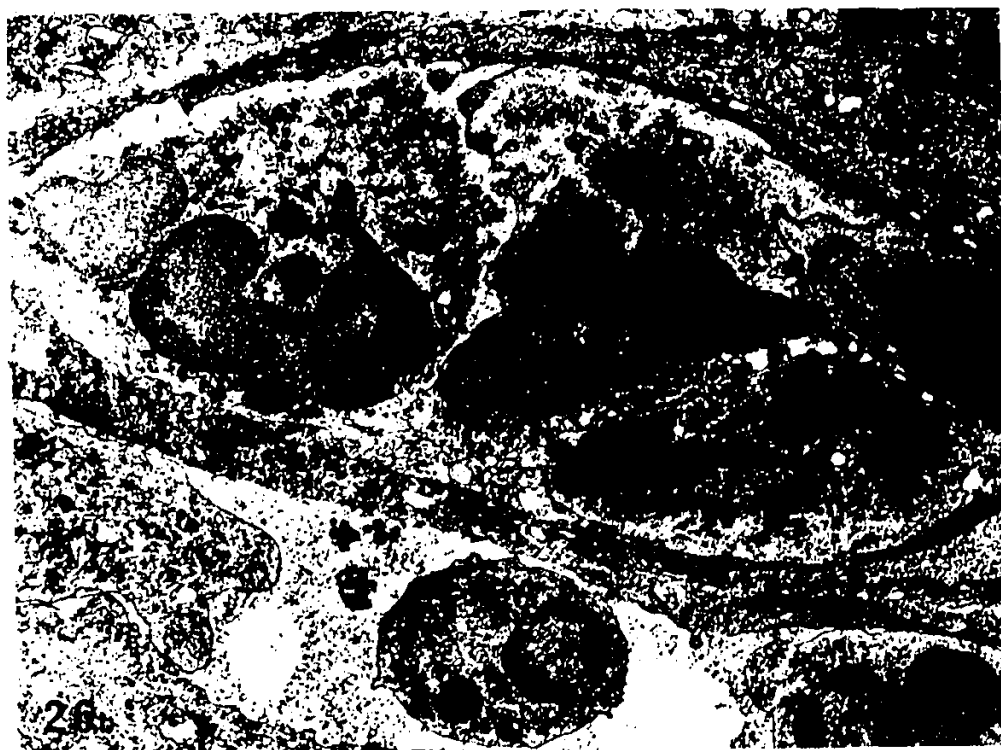


Figure 27 TEM. RA treated epidermis, 1% RA, 3 days: (a) Polymorphonuclear leukocytes (p) associated with a breach of the basal lamina (area indicated by arrow; enlarged in Fig. 27 (b)). Intercellular space (IS). 9,167x

(b) The basal lamina is disrupted in two locations (arrows) where elaborations of the basal keratinocyte plasma membranepass across the basal lamina; the largest of these is in close contact with a migrating polymorphonuclear leukocyte (P). 42,500x

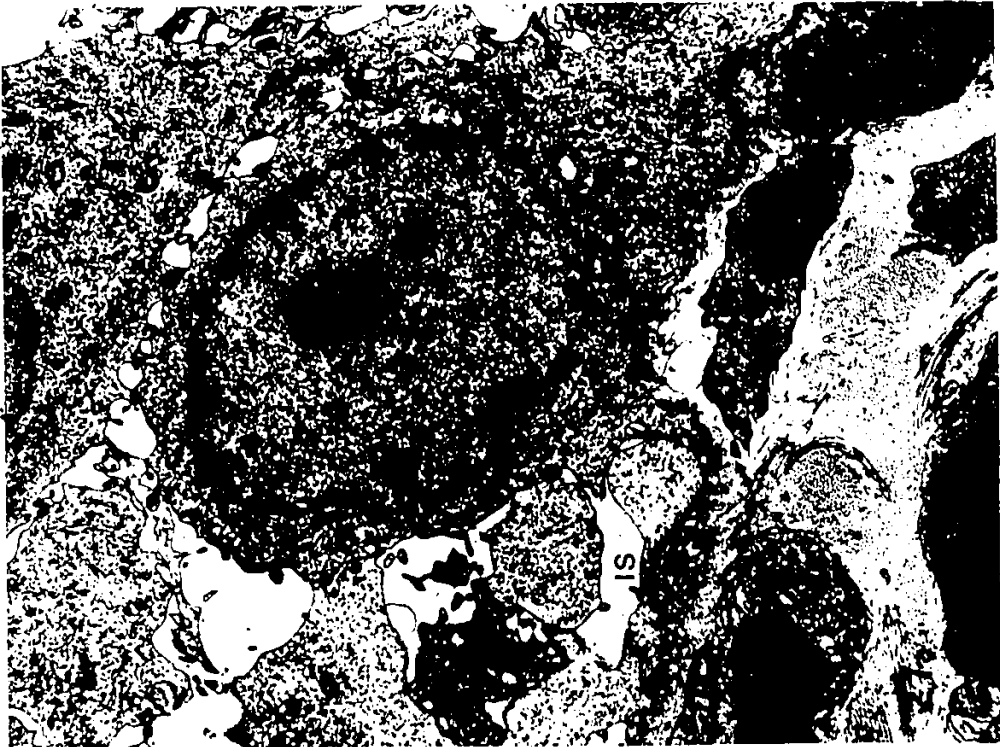


Figure 28 TEM. RA treated epidermis, 18 RA, 6 days.
Intra-mitochondrial inclusions (I), lipid-like droplets (L).
41,829x



Figure 29 TEM. RA treated, EDTA-separated, OsO₄ fixed epidermis. 0.3% RA, 6 days. Lipid-like droplets are prominent in all supra-basal layers. 5,500x



Figure 30 TEM. RA treated, EDTA-separated, OsO₄ fixed
epidermis: {

(A) 0.3% RA, 4 days. 3,300x

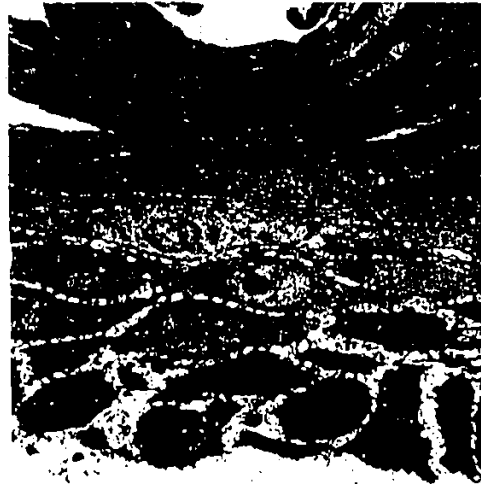
(B) 0.3% RA, 6 days. 1,762x

(C) 1% RA, 4 days. 2,933x

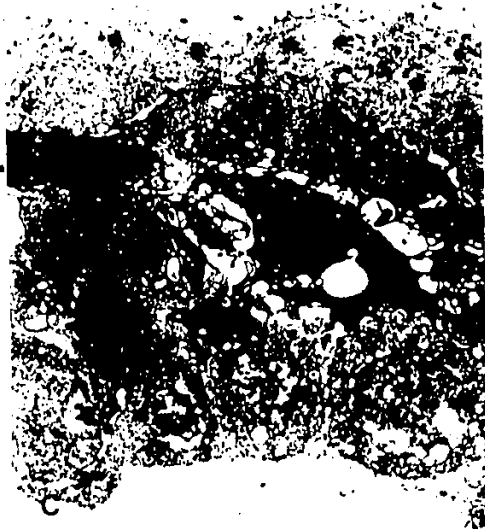
(D) 1% RA, 6 days. 1,846x



A



B



C



Figure 31 TEM. RA treated epidermis, EDTA-separated, OsO4 fixed epidermis: (a) 1% RA, 4 days. Hemidesmosomes on the ventral surface of a basal keratinocyte; note the dilated intracellular cisternae. 37,917x

(b) 0.3% RA, 6 days. Lipid-like droplet (L) in the cytoplasm of a keratinocyte in the stratum spinosum. Nucleus (N). 29,721x

(c) 1% RA, 4 days. Intercellular membrane elaboration and vacuolization in the stratum spinosum. 20,914x

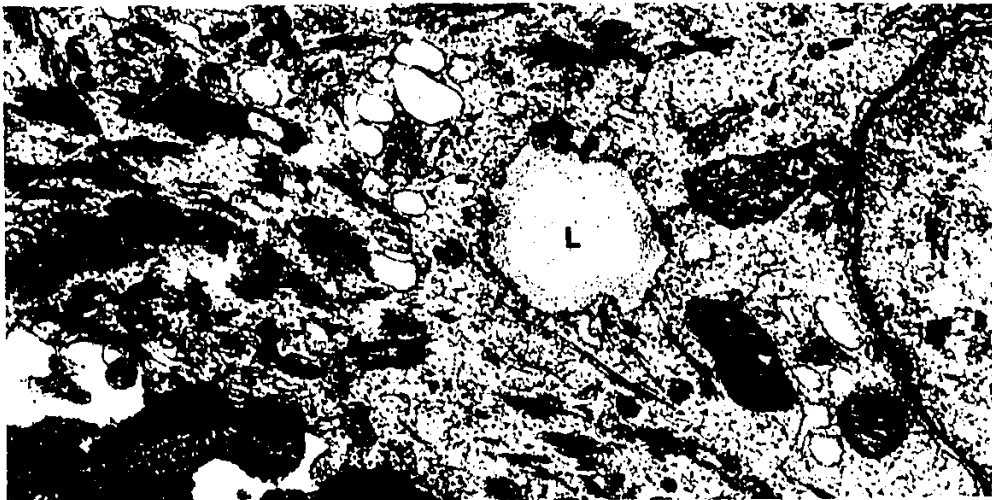
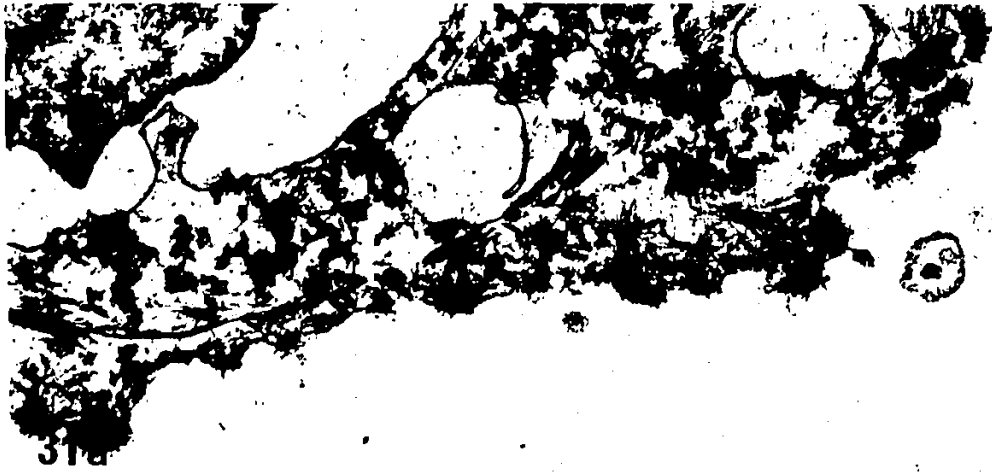


Figure 32 TEM. RA treated, EDTA-separated, OsO₄ fixed epidermis:

(A) 0.3% RA, 4 days. Blebbing of the ventral surface of a basal keratinocyte; organelles are absent and the surrounding membrane is disrupted in two locations (arrows).

12,075x

(B) 1% RA, 4 days. Membrane vesicles after release from overlying keratinocytes; the larger vesicle includes small cytoplasmic vacuoles. 11,429x

(C) 1% RA, 4 days. Membrane vesicle with many included membrane-bound vacuoles. two other (arrows) vesicles may represent an advanced stage of degeneration. 11,200x

(D) 0.3% RA, 6 days. Vesicles are surrounded by varying thickness' of cytoplasm and may arise from tube-like elaborations of the cell surface (arrow), seen here in oblique section. 12,660x

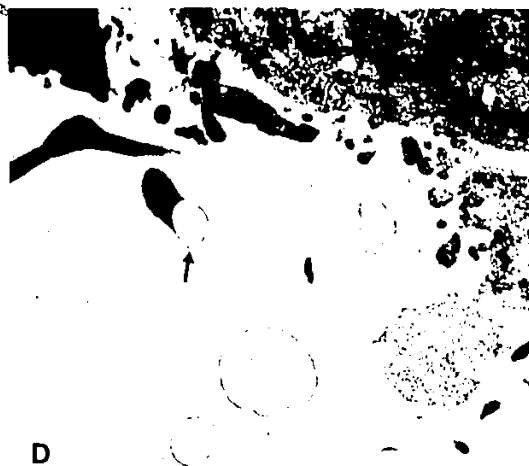
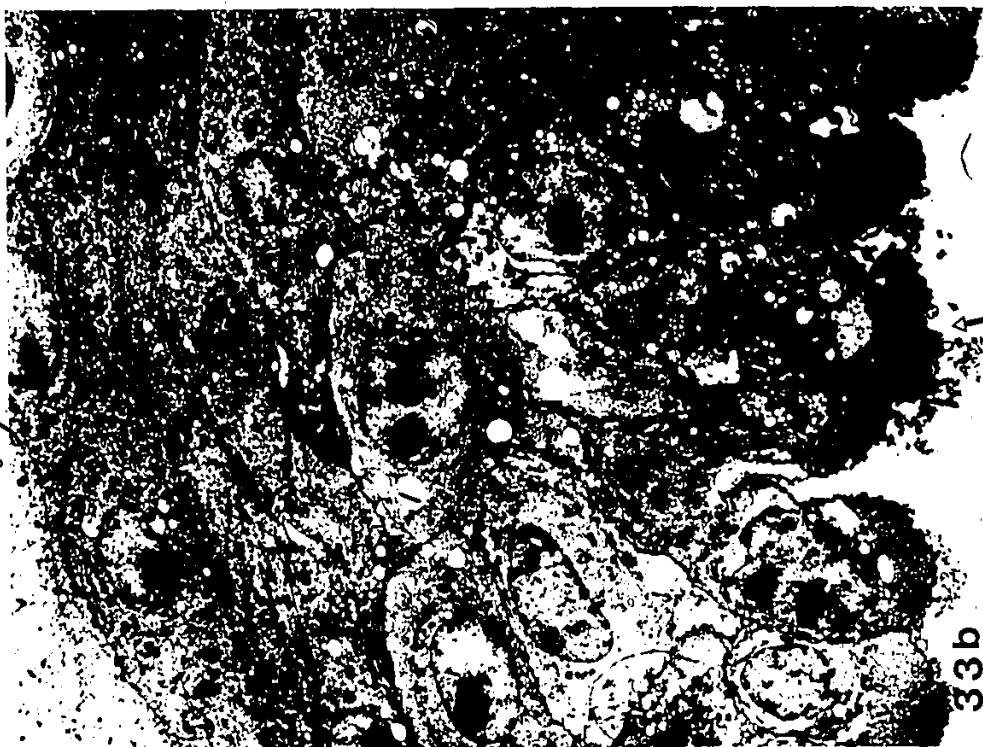
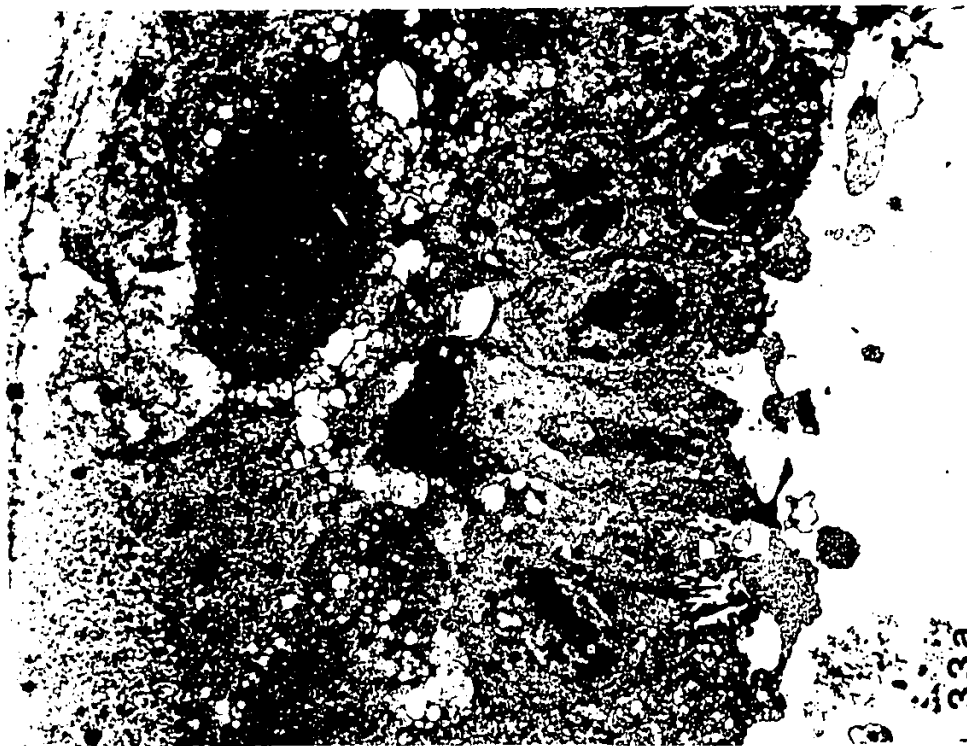


Figure 33 TEM. RA treated epidermis, EDTA-separated, RR fixed epidermis: (a) 1% RA, 4 days. Section is not contrasted with uranyl acetate or lead citrate. Vesiculation (cell surface blebbing) is abundant along the basal surface and is accompanied by intracellular penetration with RR. 3,514x

(b) 0.3% RA, 6 days. Section contrasted with uranyl acetate and lead citrate. Basal cells uniformly possess a large area of RR dense, organelle-free cytoplasm extending downwards from the ventral surface. RR penetration in the upper layers serves to illustrate the complexity of intercellular keratinocyte associations. A degenerate keratinocyte (arrow) shows very dense intracellular staining. 4,840x



33b



33a

Figure 34 TEM. RA treated, EDTA-separated, RR fixed epidermis:

(A) 0.3% RA, 3 days. Although density is poor, RR is most prevalent in the newly released membrane vesicle 11,200x

(B) 0.3% RA, 6 days. Section is contrasted with uranyl acetate and lead citrate. RR is present on the external plasma membrane surface and in the organelle-free basally oriented cytoplasm. 13,715x

(C) 1% RA, 4 days. RR is present on the external cell surface and within the newly released membrane vesicle; RR is not present in the cytoplasm of the overlying keratinocyte. 19,526x

(D) 1% RA, 6 days. RR staining patterns are similar to those described in Fig. 34 (C). 14,078x

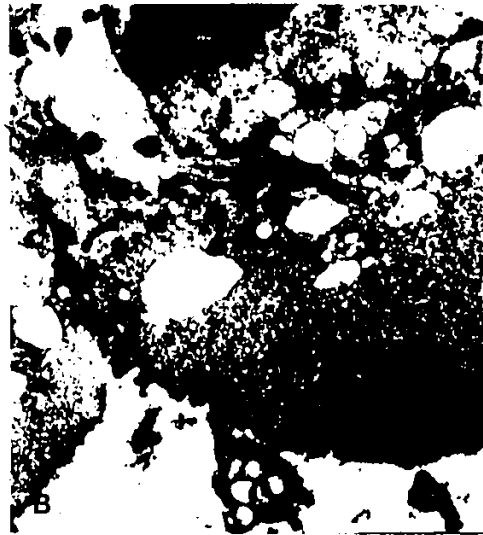


Figure 35 TEM. RA treated, EDTA-separated, RR fixed epidermis; 0.3% RA, 6 days. RR decoration of lamellated plasma membranes in the stratum spinosum. 23,200x



Figure 36 TEM. RA treated, EDTA-separated, RR fixed epidermis; 0.3% RA, 6 days. Membrane coating granules in the upper stratum spinosum releasing their contents into the intercellular space. Desmosome (D). 90,846x.

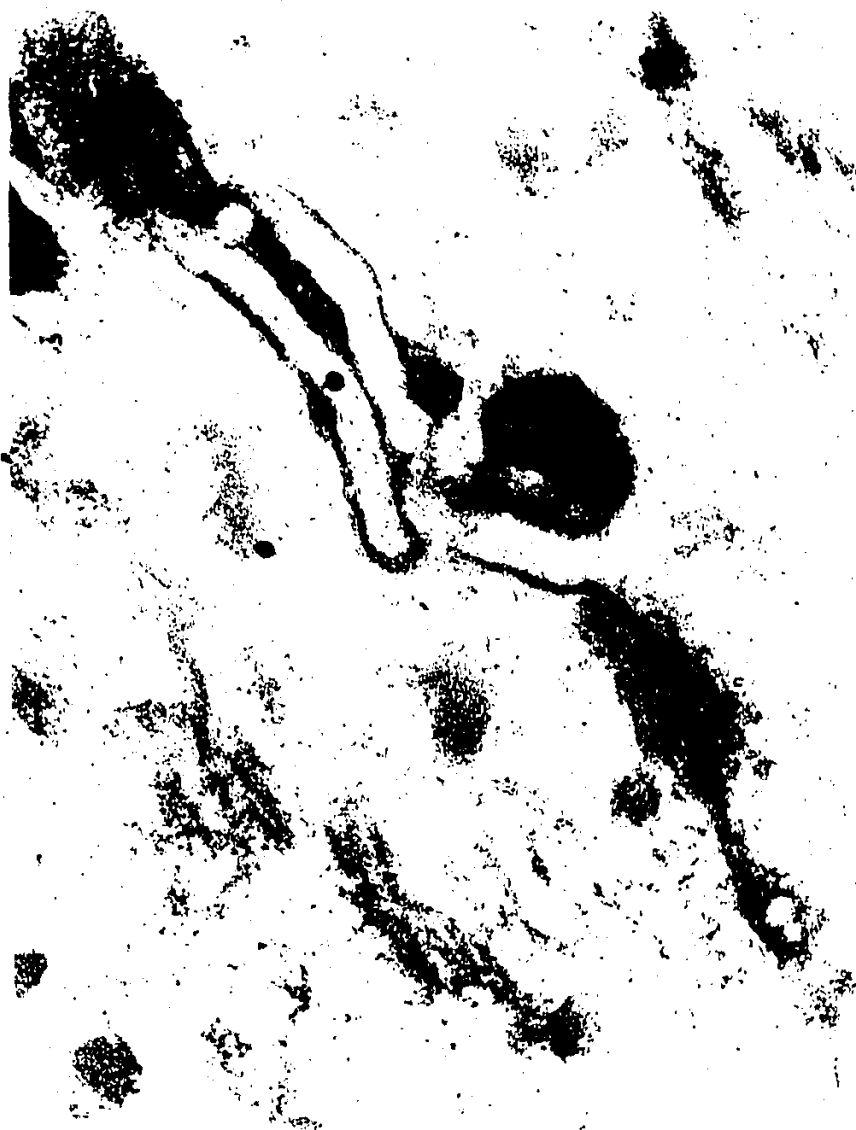


Figure 37 SEM. RA treated, EDTA-separated epidermis: (a) 0.3% RA, 1 day. Inter-follicular basal epidermis with abundant LCs; hair follicles can also be observed. 446x
(b) 0.3% RA, 4 days. Inter-follicular basal epidermis; LCs, if present, are obscured by abundance of overlying membrane vesicles and cell debris. 1,348x

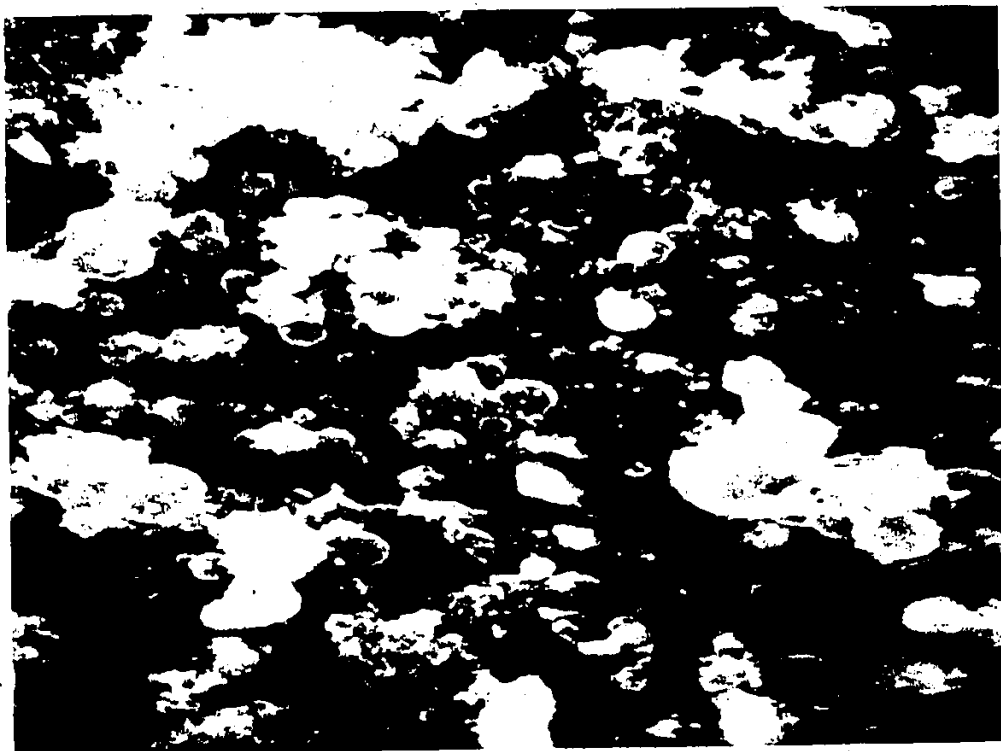
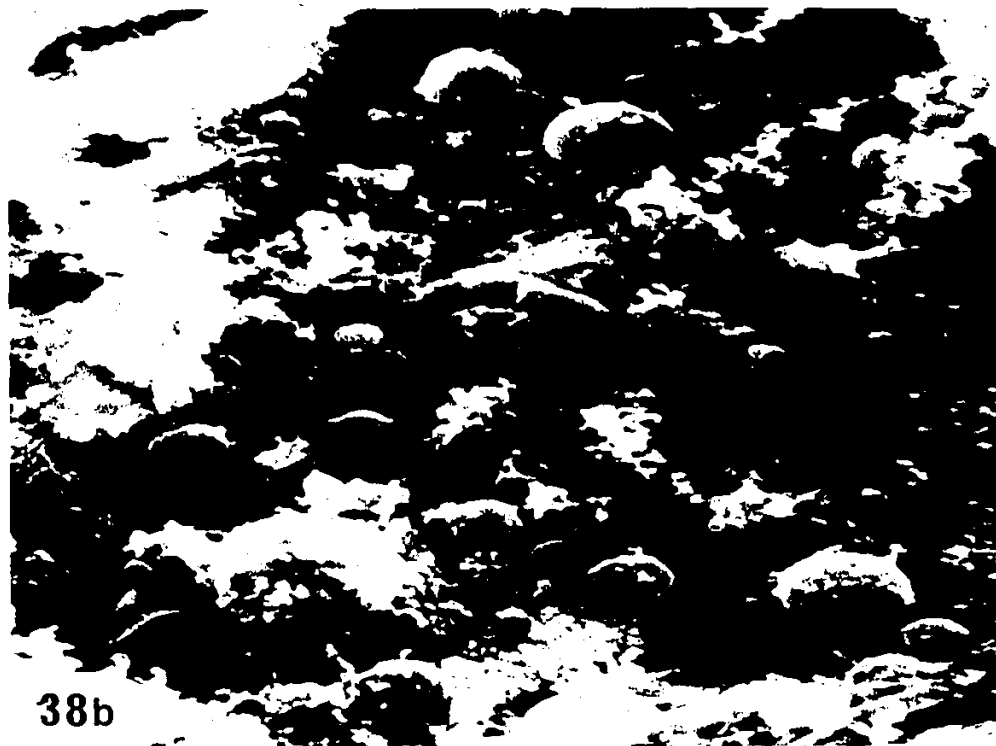
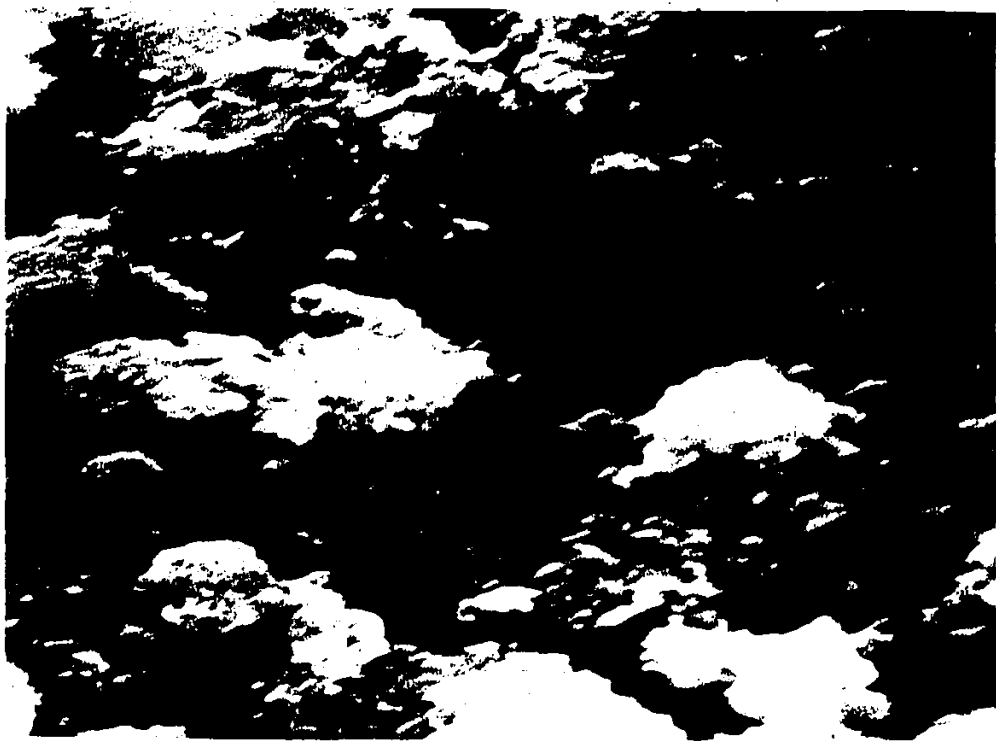


Figure 38 SEM. RA treated, EDTA-separated epidermis: (a) 1% RA, 4 days. Basal keratinocytes are separated by enlarged intercellular spaces. 2,935x
(b) 1% RA, 8 days. The intercellular space is diminished in size and membrane vesicles are relatively abundant. 3,130x

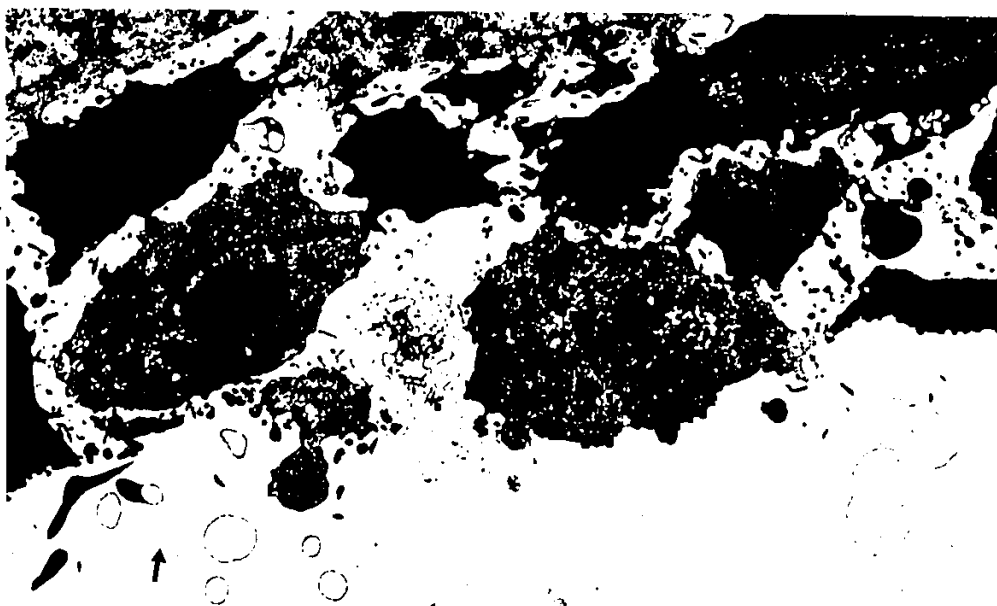


38b

Figure 39 RA treated, EDTA-separated epidermis, 0.3% RA,
6 days: (a) TEM. Basal epidermis after EDTA separation; the
area indicated by the arrow is enlarged in Fig. 32- (A).

7,333x

(b) SEM. Three-dimensional perspective on basal epidermis
treated as in Fig. 39(a). 2,038x



39a

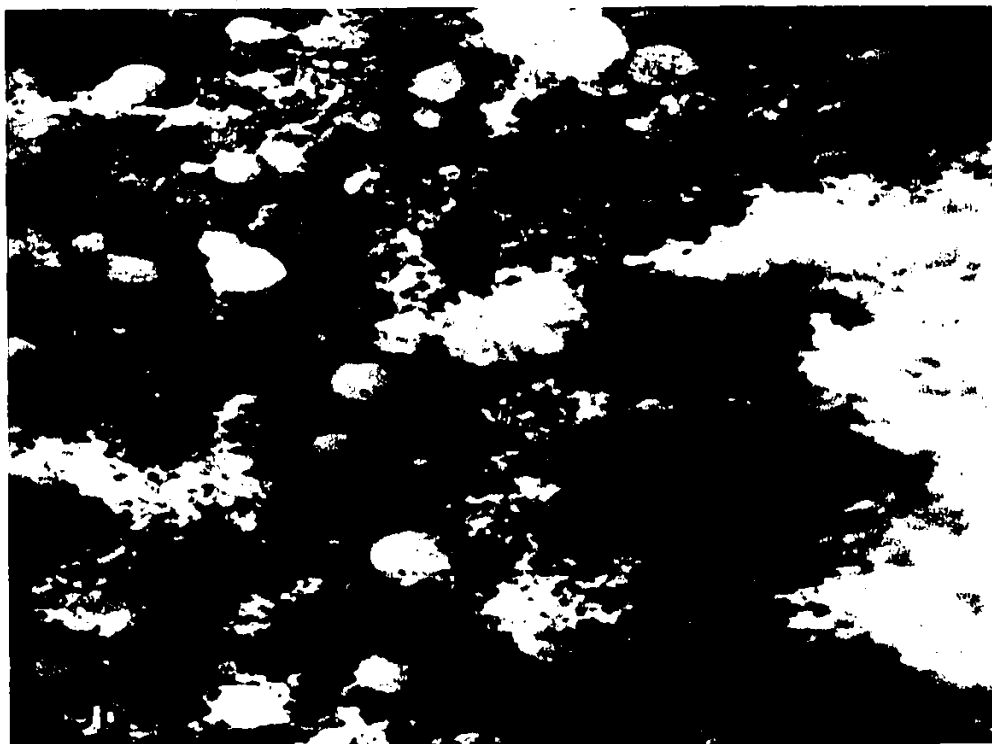


Figure 40 SEM. RA treated, EDTA-separated epidermis, 0.3% RA, 8 days: (a) Basal keratinocytes, abundant cell blebbing, numerous membrane vesicles and enlarged intercellular spaces; membrane vesicles are often continuous with underlying keratinocytes (arrows); the area indicated by the double arrows is enlarged in Fig. 40 (b). Note the presence of desmosomal projections on the otherwise smooth lateral cell surface (star). 4,280x

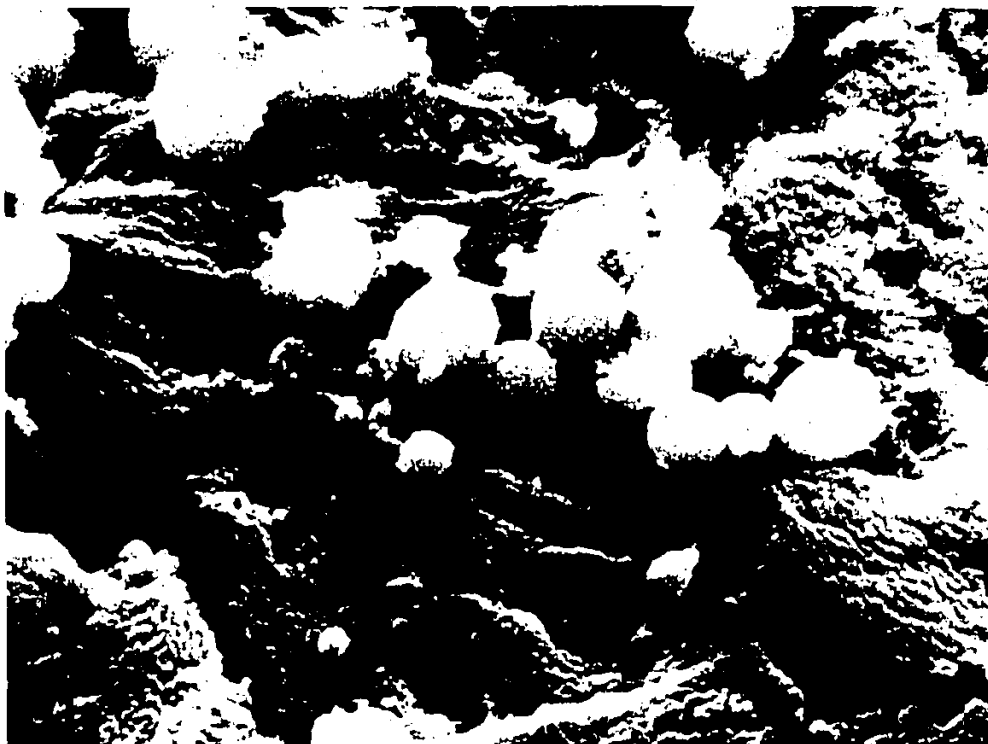
(b) Enlarged from Fig. 40 (a). A tube-like extension of the ventral surface of a basal keratinocyte; the projection is terminated with a spherical membrane vesicle and is suggestive of internal continuity. Ridges of hemidesmosomes are abundant. 19,427x



Figure 41 RA treated, EDTA-separated epidermis, 0.3% RA, 8 days: (a) TEM. An alternate view of the epidermal undersurface after prolonged RA exposure. The area indicated by the arrow is enlarged in Fig. 41 (b). 7,079x.

(b) SEM. Hemidesmosome ridges enlarged from Fig. 41 (a). 15,408x

(c) TEM. Hemidesmosomes in cross section. 31,417x



41b




41c

Figure 42 SEM. RA treated, EDTA-separated epidermis:

(a) 0.3% RA, 8 days treatment and 14 days regeneration. The epidermis appears relatively normal. 1,761x

(b) 0.3% RA, 14 days treatment and 14 days regeneration.

1,761x



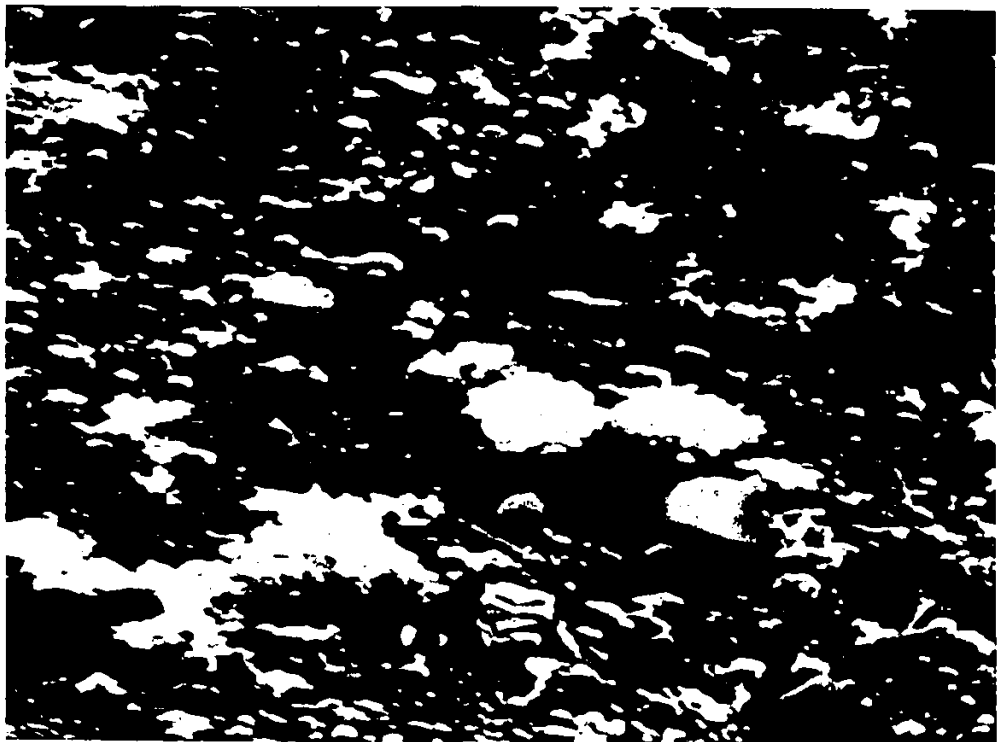
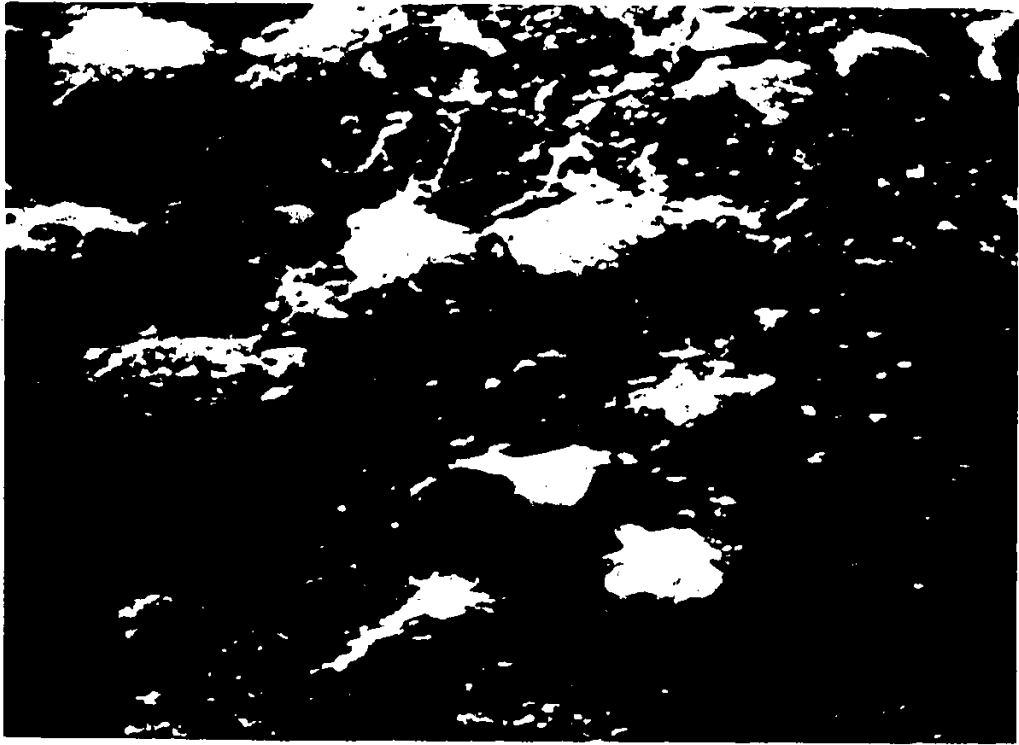


Figure 42 (cont'd from previous page)

(c) control preparation; propylene glycol, 7 days. The epidermis is unchanged. 1,878x

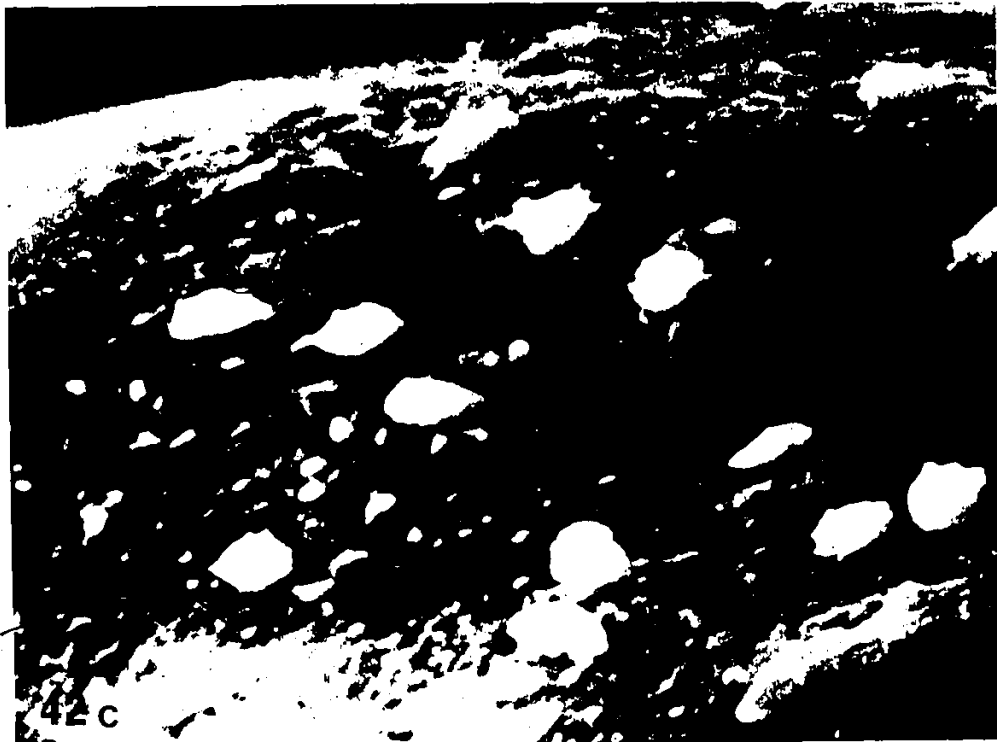


Figure 43 SEM. RA treated, EDTA-separated dermis: (a) 0.3% RA, 1 day. Surface of the basal lamina is smooth except for an even distribution of pore-like depressions. 283x
(b) 0.3% RA, 6 days. Surface of the basal lamina is extremely irregular after continued RA exposure. 1,130x
(c) 0.3% RA, 10 days. Surface of the basal lamina is returning to normal contours. 1,130x



Figure 44 TEM. RA treated, EDTA-separated dermis: (a) 0.3% RA, 4 days. Polymorphonuclear leukocytes (P) in the dermal matrix. A single disruption of the basal lamina (arrow) is closely attended by a partially visible leukocyte. 4,657x

(b) 1% RA, 4 days. Polymorphonuclear leukocytes (P) in the dermal matrix. Disruption of the basal lamina (arrow). 7,492x



DISCUSSION

General

LM observation of hairless mouse skin provides a reasonable degree of assurance that the gross tissue architecture (Figs. 1,2), at 13-20 weeks of age, is in close agreement with the earlier descriptions of Montagna et al. 1952 (2) and Orwin et al. 1967 (3). Epithelial cysts of many descriptions are frequently observed in the deeper dermis while the dissociated, inactive follicles appear plugged by an internal buildup of sebum and squames (Fig. 1).

Epidermal ultrastructure and organization (Figs. 4a,b,c) in the hairless mouse was also essentially as described in previous anatomical studies (4,83); thus confirming its reported similarity to the epidermis of the mouse with hair (4). Moreover, body wall epidermis, in the hairless mouse, possesses an even distribution of dendritic LCs positioned in the stratum basale (Fig. 4a,b,c). In comparison, human (5), guinea pig (6) and mouse footpad (7) epidermis also possess an even distribution of dendritic LCs but, positioned in a supra-basal rather than basal location. Organizationally, in all essential respects, the epidermis of the hairless mouse comprises a "reticulo-epithelial" system, as originally detailed by Shelley and Juhlin in 1976 (26).

The abundance of Langerhans granules per LC (Figs. 4b,c) would suggest that the hairless mouse, relative to man, guinea pig, and hamster, is unusual. The significance of this observation is not readily apparent at the present time as the functional importance of the Langerhans granule is unknown. It may however, become important as the relative nature of cell mediated immunity and keratinization, in the hairless mouse, becomes better understood. At present the murine immune system is very well understood (84), and may contribute to rapid advances in understanding the role played by the intra-epidermal LC. Its unique morphologic qualities, especially the cytoplasmic Langerhans granule, may correlate with a comparably specific functional distinctiveness.

Membrane ATPase activity was relatively abundant in the LC as compared with surrounding keratinocytes (Figs. 3a,b). A sequential reaction with ATP, lead, and sulfur produced an easily perceived black precipitate. Positive staining of surrounding keratinocytes has verified the quality of the enzyme reaction in the absence of stained LCs; thus, those areas lacking well stained LCs, yet possessing obviously stained keratinocytes, are either lacking enzymatically functional LCs or, are lacking LCs altogether.

Previous studies, using a similar ATPase staining reaction have quantitated LC populations from different species and from a variety of anatomical sites, both normal and treated (6,7,12,36,85,86,87,88,89). Some of these

studies (85,87,88,89) however, using mouse epidermis, have failed to properly consider extremely relevant criteria in the evaluation of their statistical results. ATPase staining for example, although clearly demonstrating LC morphology in the present study, must be considered quantitatively, with serious reservations, primarily because of the inherently equivocal staining characteristics of murine epidermal sheets; staining of individual epidermal sheets was frequently variable in the best of preparations after a variety of staining regimens. Rowden has confirmed this observation with reports of similar ATPase staining problems using murine epidermal sheets from a variety of mouse strains (90). Mouse epidermis, because LCs are located so close to the basal lamina, may be more sensitive to the disruptive effects of EDTA separation and ATPase staining and thus, a poor model for quantitative LC studies using such techniques. In future studies, the question of LC depletion as artifact would be well addressed using histological analysis to supplement ATPase quantitations.

Furthermore, LCs, relative to surrounding keratinocytes, were clearly mobile after separation of epidermis and dermis with EDTA. The extrusion (Fig. 9b), or more appropriately, the migration of intra-epidermal LCs occurred regularly, with cell bodies and cell processes commonly observed external to the overlying epidermis (Figs. 6,7a,8a,b,9a,b,13a,b,15a,b,16a,b). Alternatively--though it seems only a partial explanation--LCs may have been exposed

incidentally as a function of EDTA damage to surrounding basal keratinocytes. LCs were ultrastructurally well preserved yet show marked changes in their shape, orientation and the nature of cell surface elaborations. Most were wholly or partly externalized, cell bodies gave the appearance of flowing and external LCs were distinctly different from their intra-epidermal counterparts. The appearance of LC movement supports the view that LCs may migrate in and out of the epidermis, not only during embryonic development (28), but also in response to external stimulation as proposed by Silberberg 1973 (25).

The disodium salt of EDTA (20 mM) was used in the present study instead of the tetrasodium salt (20 mM) used in previous studies. The physical separation of dermis and epidermis was easily undertaken, as described by those authors using $\text{Na}_2\text{-EDTA}$ (7,33,34). EDTA separation specifically, occurred within the lamina lucida, an electron lucent zone lying between the basal lamina and overlying keratinocytes (Fig. 5). This is in agreement with the observations of Scalletta and MacCallum, 1972 (33). However, using 2 hrs. incubation, at 37°C , the epidermis was somewhat different in the ultrastructural character of basal keratinocytes. The majority of hemidesmosomes were engulfed, withdrawn into the cytoplasm, and often remained in a perinuclear location (Figs. 6,7a,b). In comparison, Scalletta and MacCallum (33) describe only infrequent

hemidesmosome engulfment in EDTA separated human epidermis.

It can be concluded that the bulk of ultrastructural change in mouse epidermis occurs during EDTA incubation, and not as a function of mechanical separation or exposure to subsequent buffer washes and fixatives. This is well illustrated by two consistent observations (i) ultrastructural changes (hemidesmosomal engulfment, perinuclear accumulation of organelles, microvilli formation) were observed in skin left intact (Fig. 5), and fixed directly in OsO₄ after 2 hrs incubation in 20 mM EDTA. (ii) Ruthenium red fixation shows obvious decoration of external hemidesmosomes and a total absence of hemidesmosome staining within cytoplasmic vacuoles (Figs. 7a,b,33b,34b); hemidesmosomes therefore, were invaginated prior to fixative exposure.

In comparing the changes elicited by EDTA in the murine system, with changes occurring in human skin, one must consider their inherent morphological differences. Most significantly, the subcutaneous fat layers are comparatively thin in the mouse, as is the overlying epidermis. It may be that EDTA penetration and subsequent damage is relatively limited by these layers, thereby reducing the hemidesmosomal engulfment observed in EDTA-separated human epidermis. However, one has difficulty consolidating this view with the fact that EDTA separations are possible after only 1-1.5 hrs. with human (33) and guinea pig (6,36) epidermis, as compared with 2 hrs. in the hairless mouse.

In this regard, the total thickness of the epidermis may also affect the mechanics of EDTA separation. In man and guinea pig, for example, the epidermis is relatively thick and substantially more durable (under mechanical stress), as compared with mouse. The mechanical stability of these thicker epidermal sheets would ensure greater durability during the delicate procedure of mechanical separation of dermis and epidermis. The application of increased pull during mechanical separation may allow the event to take place after shorter periods of incubation.

Furthermore, hairless mice possess hair follicles which seldom open to the surface due to substantial accumulations of sebum and squames. These accumulations may significantly limit the hair follicle as a means of EDTA access to those areas of adnexal cell adhesion to the dermal substrate. Humans and guinea pigs, in comparison, possess externally available hair follicle passages which penetrate deeply into the dermis. In such systems, the hair follicles would be quickly liberated from the dermis, via improved EDTA access, allowing an easier mechanical separation overall. EDTA separation in the hairless mouse, however, may be slowed by reduced penetration within the hair follicles, while EDTA access to the interfollicular epidermis would be relatively abundant, and thus, potentially more damaging.

Cation deprivation affects not only the specific

adhesion between basal keratinocyte and the dermal matrix, but has also disrupted the integrity of cellular structures associated with the epidermal-dermal junction. At the subcellular level this has proven to be a remarkable benefit in the morphological characterization of hairless mouse epidermis. LCs, which normally inhabit a basal location--separated from the basal lamina by thin process' of adjacent keratinocytes--migrate, or are extruded down and outwards after EDTA elicited contraction of surrounding keratinocytes. As such, LCs remain easily available for correlative microscopic observation (Figs. 8, 13a, 15a, b).

Previous studies (34, 91, 92), using a variety of separation techniques, have used SEM to examine the epidermis from this inverted perspective. All three have examined human epidermis after sodium bromide separation, an extremely harsh technique due to the severe osmotic and pH differentials between tissue and separating solution. Although some EDTA separated tissue was examined, it was not extensively discussed (34). Gross comparison however, of the epidermal undersurface from humans with that of the hairless mouse, serves very well in demonstrating basic differences between the two. Hairless mouse skin lacks the very deep and obscuring dermal papillae seen in human skin (34, 91, 92). Melanocytes also, are not observed in mouse epidermis yet are relatively common in the basal layers of human epidermis; melanocytes are described by Papa and Farber (91) and Drzwiecki and Kjaergaard (34), although both authors

fail to address the possibility that these dendritic cells may, in some cases, be LCs. Furthermore, Drzwiecki and Kjaergaard (34) conclude that Dopa stained epidermal sheets reveal dendritic cells that are partially charged as a function of internal melanin content. This charge may in fact be a simple function of the cell's elevated position as it rests on, and partially between surrounding keratinocytes. Physical release of exaggerated secondary electron emissions is a common observation when a sample possesses such protruding contours. The LC population discussed in the present study is clear evidence of this kind of charging artifact.

Many studies, as described, have microscopically examined epidermis after separation from it's dermal counterpart. However, none of these previous studies examines hairless mouse epidermis, nor do they utilize the high resolution SEM, as does the present study. Thus, the correlative microscopic analysis of epidermal subcellular organization in this model is thus far, the first documented presentation of such information. Moreover, the normal subcellular structure and organization is well established for continuing comparison with RA treated epidermis.

The dermis, after EDTA separation, was well preserved in all microscopic preparations. Three dimensional SEM structure was generally unremarkable except in confirming the uniformity of epidermal-dermal separation and verifying the sheet like structure suggested by TEM cross-sectional preparations (Figs. 10, 12a,b,c, 13b).

Epidermis and dermis fixed with RR as a ligand of OsO₄ revealed abundant filamentous material on the external surface of all observed cells, and the basal lamina (Figs. 7a,b, 10c). This observation is particularly evident in the SEM preparations which were examined without the aid of a conductive metal coating (Figs. 15a, 16b). The filamentous material probably represents the glycocalyx of the keratinocyte plasma membrane, as described by Luft in 1971 (38).

RR-OsO₄ permits morphological characterization in the SEM without prior application of a conductive metal coating. It's overall utility however, seems suspect in view of the fuzziness of the glycoprotein matrix and the extent to which underlying structure is obscured.

Babaii (40) and Luft (38) have suggested that RR fixation and staining may act as a monitor of membrane damage and cell viability. This has been well illustrated in the present study where RR has served as a useful probe for:

- (i) plasma membrane permeability changes occurring in newly

separated basal keratinocytes (Figs. 7a,b,33a,b,34a,b,c,d);
(ii) increases in intercellular permeability (Figs.
7a,b,33a,b,35,36).

After RA treatment, RR was commonly observed in the cytoplasm of basal keratinocytes (Fig. 33b) and in newly formed membrane vesicles. Vesicles, either free or attached (Figs. 33b;34b), appeared to occur as a function of RA-EDTA induced membrane permeability. Basal cells released membrane vesicles after penetration by, and swelling with, external materials. This probable sequence is suggested by the fact that RR appeared only in enlarged portions of the ventral cell body (Figs. 33b;34b) and in adjacent or closely associated membrane vesicles (Figs. 34c,d). In comparison, RR penetration was lacking in the cytoplasm of cells which had just released membrane vesicles; such cells were resealed, ultrastructurally sound and impermeable to RR. Clearly, RA has changed the basal keratinocyte plasma membrane response to EDTA separation and this in turn has resulted in substantial cell damage as a function of enhanced membrane permeability.

In TEM preparations of RA treated epidermis, intercellular penetration and staining with RR (in EDTA separated tissue) revealed a variety of extremely complex interdigitating cellular associations amongst high level keratinocytes (Fig. 35). These complex structures were not readily apparent in tissue fixed solely with OsO₄, either whole or EDTA-separated. Moreover, the complexity of cell to

cell adhesion revealed in this manner, suggests that epidermal cells may be compensating for the reduction in mechanical stability created by an absence of desmosomes.

The glycoprotein nature of membrane coating granules (93), their extracellular continuity (94), and their fine structure and organization (93,94,95) were also particularly well illustrated by RR (Fig. 36).

RR is thus, a potentially useful stain for mapping intercellular associations in organizationally compact tissues such as the epidermis. It also provides a useful staining probe for the characterization of certain membrane associated secretory structures.

Retinoic Acid

Generally, RA has elicited specific epidermal responses that have been previously described in earlier reports. Markers of orthokeratinization (an evenly layered stratum corneum, membrane coating granules, keratohyalin granules, tonofilaments, and desmosomes) are initially reduced, both in the apparent extent of their individual size and prominence, and in their overall occurrence. These changes were observed in varying degrees, and at different times during the short term intensive application of 0.3% and 1% RA. The epidermal response was more intense after exposure to 1% (Figs. 19a,b,30c,d) as compared with 0.3% (Figs. 18c,d,30a,b) RA. Concomittant with an apparent reduction in keratinizing markers was a clear shift--again dose dependant--in the metabolic direction of differentiating epidermal cells. RER (Figs. 24b,c), Golgi stacks and vesicles (Figs. 22c,24a), sequestered lipid (Figs. 21a,c,d,24c,28,31b), and sparse glycogen deposits (Fig. 24b) occur in unusually large quantities.

Although the above changes agree with similar studies using topical RA, the obvious conclusion, that such changes are specific to RA, is somewhat suspect. RA has often been described as exerting an anti-keratinizing effect because of the following: squamous metaplasia occurring during vitamin A deficiency (51), the elicitation of mucous secretion amongst cultured epithelial cells (keratoacanthoma,

embryonic chick skin) (71,72,73,96), the reduction of keratinizing elements, in vitro using cultured skin explants (50), and in vivo using human (77), guinea pig (50,78), and mouse skin (45,79), and finally, the beneficial therapeutic effects observed in the treatment of various scaling and acneiform dermatoses (97). Clearly, RA and R are systemically active in the maintenance of a variety of epithelia, probably by limiting the rate and degree of squamous metaplasia. However, when one examines in vitro and in vivo situations where R and RA effects are not mediated by specific transport and receptor proteins (such as in this present study, which uses topical applications of pharmacological concentrations of RA) a distinction must be made; between general toxic effects and non-toxic, presumably tissue specific physiologic mechanisms.

Glycogen for example, has frequently been observed scattered throughout the cytoplasm of RA treated keratinocytes (45,50,77,78,81). Glycogen accumulation has also been observed after UV irradiation (98), tape stripping (45), wounding (99), application of irritant chemicals (100) and carcinogens (101). Lipid droplets, although sometimes present in the cytoplasm of normal keratinocytes, are extraordinarily abundant in the upper epidermis and stratum corneum of RA treated hairless mice, as previously described by Christophers and Wolff (50,78) using guinea pig epidermis. Lipid droplets have also been observed in response to ethanol (45), irritant compounds (100), and UV

irradiation (98). They appear in psoriasis and a variety of scaling disorders as well (102,103,104,105).

Intramitochondrial inclusions (Figs. 23c,24b,c,25,28), widened intercellular spaces (Figs. 22a,b,c,d;25,29), microvillous projections of the plasma membrane (Figs. 22a,b,c,d), and disruption of desmosomal associations (Figs. 22b,c), as described in the present study, have also been reported to occur in the epidermis after a variety of treatments (45,98,100,101,106,107,108,109,110). The shift in epidermal metabolism and differentiation indicated by these ultrastructural changes, in combination with enhanced development of Golgi and RER, suggests a short term detoxifying response. In this regard, one is impressed by the general organizational similarities between the cytoplasm of RA treated keratinocytes (Fig.24a) and normal hepatocytes.

On-going ultrastructural studies in this laboratory are investigating the epidermal irritant response produced by topical application of 1% DNCB, a contact irritant: the changes observed are strikingly similar to those elicited by topical application of RA. Epidermal cell division and cell transit time are elevated while normal patterns of keratinization are displaced by epidermal metaplasia leading to the formation of lipid-containing parakeratotic scale.

When all relevant observations are considered in terms of differentiating between the physiologic role of RA relative to its toxic effects, it may be speculatively

concluded that the majority of changes stem from its toxic irritant effects. Its true physiologic effects may well be obscured by the enormity of such toxic change.

Future studies of a more rigidly biochemical nature might confirm or deny the suggestion that topical application of RA, like DNCB, carcinogens, tape stripping, and UV light, induces metabolic pathways oriented towards processing and elimination of potentially injurious materials. The use of radiolabeled compounds would allow monitoring of the relative distribution and metabolism of topically applied RA, both intra- and extracellularly. One might suspect that, in the present study, the metabolized forms of RA, as described by DeLuca (52), or its conjugate, anabolic forms, as described by Wolff (65), would appear in increasing amounts over time as a function of increased epidermal metabolic capability; on a time scale this would probably coincide with the return of normal patterns of keratinization and an increase in epidermal thickness and cellularity.

The present study fails to monitor the long term (14 days) changes occurring after the intensive application of RA, and as such may observe only short term toxic change. Kaidby, Kligman, and Joshida (77) have studied such a long term response in human skin. Their LM observations describe an acute dermatitis response up to 14 days with application of 0.3% RA, which resolved to a near normal appearance after 40 days continuing exposure. After 40 days the permeability

of the skin was markedly enhanced due to diminished adherence of external corneocytes and, paradoxically, inherent skin sensitivity to specific molecular antigen was decreased (one would expect an increase in sensitivity as a function of increased epidermal permeability). These relatively minor changes may represent the physiologic effects of epidermal exposure to elevated levels of free RA.

Ultrastructural analysis of tissue treated with RA for more prolonged time periods may provide additional clues to the nature of epidermal resiliency in the face of toxic stress. Furthermore, the suggestion by Kaidby (77), that clearance of RA (and topical antigen) via the dermal vasculature is increased after long term application, could then be investigated by quantitative analysis of radiolabeled RA in the serum, liver, and excrement.

The present study, using 0.3% RA, shows generally normal patterns of keratinization after 10-14 days, instead of the 40 days reported by Kaidby (77). These results, using a considerably different epidermal model and showing relatively normal epidermis after 14 days continued exposure, may in fact, represent the same epidermal response observed by Kaidby after 40 days. If such is the case, prolonged RA treatment and observation in the hairless mouse would be redundant and unenlightening.

In SEM observations of RA treated epidermis, it is of

key importance to note that subcellular differences between treated and untreated samples are directly related to subcellular responses to EDTA separation, fixation, and critical point drying. Thus, one cannot state, "this is what a basal keratinocyte looks like", but rather, must add the qualification, "this is what a basal keratinocyte looks like after EDTA separation, fixation, and critical point drying". With this limitation in mind however, the comparison remains nonetheless insightful, and clearly illustrates marked differences between RA treated and untreated epidermis.

In normal epidermis, hemidesmosomes are invaginated and appear intracellularly, while treated epidermis shows a clear array of hemidesmosomes in their original, basal membrane location (Figs. 29, 30a,b,c, 32a,b,c,d). Ultrastructurally, in both whole and EDTA separated tissue, RA causes a reduction in tonofilament-hemidesmosome associations (Figs. 25, 27a,b, 41a,b,c). Accordingly, the interaction of filaments and hemidesmosomes may permit invagination in normal epidermis and, due to a lack of tonofilament-hemidesmosome integrity, limit such invagination in RA treated tissue. Alternatively, since mg^{++} interaction with the cytoskeletal network is known to affect intracellular contractile activity, it may also be involved in the invagination of hemidesmosomes in normal epidermis. Such an event may be directly affected by the increased permeability of the plasma membrane after RA treatment. Clearly, the barrier function is reduced, as indicated by

the abundance of cell blebbing, vesicle formation (Figs. 39a,b,40a,b) and the increase in RR penetration (Figs. 33b,34a,b,c,). Chelation of intracellular mg^{++} and ca^{++} would be potentially enhanced, possibly eliminating any subsequent cytoskeletal contractile activity and thus preventing hemidesmosome invagination in RA treated epidermis. Both explanations, concerning RA induced changes, are somewhat speculative in nature and remain largely unsupported by any additional confirming evidence other than that described.

RA induced changes in basal cell membrane surface structure, and concomittant cell blebbing, tentatively support the view that plasma membrane structure, function and probably synthesis are significantly altered as a function of prolonged RA application.

APPENDIX I

FIXATIVES

Dalton's Fixative

Preliminary

Prepare 2.5 N KOH solution; 14 g KOH / 100 mls. H₂O.

Prepare 3.4% NaCl solution; 8.5 g / 250 ml. H₂O.

Potassium dichromate buffer

Add 10 g potassium dichromate to 200 ml. H₂O. Using 2.5 N KOH, adjust Ph to 7.4. Add 250 ml. of 3.4% NaCl solution.

Add 250 ml. glass distilled H₂O and store at 4 C.

Fixative

Dissolve 1.0 g OsO₄ in 50 ml. H₂O and add 50 ml. dichromate buffer.

Fixation

Fix tissue for 2 hours at 4 C.

Ruthenium Red-OsO₄ Fixatives

Preliminary

Prepare a 5% gluteraldehyde solution; dilute 10 ml. 8% gluteraldehyde (polysciences) with 6 ml. H₂O.

Prepare 1% ruthenium red solution; 0.1 g RR / 100 ml. H₂O.

Prepare 0.2 M cacodylate buffer; add 21.4 g sodium cacodylate (sigma) to 500 ml. H₂O. Adjust to pH 7.3 with 1 N HCl.

Prepare cacodylate (0.1 M) buffered 0.5% ruthenium red solution; 5 ml. 1% RR / 5 ml. 0.2 M cacodylate buffer.

Prepare 2% OsO₄ solution; 1 g OsO₄ / 50 ml. H₂O.

Fixatives

(a) Cacodylate (0.1 M) buffered gluteraldehyde (2.5%); 16 ml. 0.2 M cacodylate buffer / 16 ml. 5% gluteraldehyde.

(b) Cacodylate (0.1 M) buffered 1% OsO₄-0.05% RR; 18 ml. 0.2 M cacodylate buffer / 18 ml. 2% OsO₄ / 4 ml. 0.5% RR.

(c) Cacodylate (0.1 M) buffered 1% OsO₄; 15 ml. 2% OsO₄ / 15 ml. 0.2 M cacodylate buffer.

(d) Ruthenium red (1%) in H₂O; 2 ml. 1% RR / 18 ml. H₂O.

(e) OsO₄ (1%) in H₂O; 50 ml. 2% OsO₄ / 50 ml. H₂O

Fixation

Fixation was at 4°C.

Fix: (a) 1 hr. in cacodylate (0.1 M) buffered gluteraldehyde (2.5%);

(b) 3 hrs. in cacodylate (0.1 M) buffered 1% OsO₄-0.05% RR;

(c) 1 hr. in cacodylate (0.1 M) buffered OsO₄ (1%);

(d) 1 hr. in RR (1%) in H₂O;

(e) 1 hr. in OsO₄ (1%) in H₂O.

Bouin's Fixative

Prepare fixative; picric acid (supersaturated solution)- 75 ml. / formalin- 25 ml. / glacial acetic acid- 5 ml..

Fixation:

Leave in fixative overnight at room temperature.

APPENDIX II

ADENOSINE TRIPHOSPHATASE SOLUTIONS

Tris-maleate buffer

tris(hydroxy methyl)amino methane- 2.42 g

maleic acid- 1.96 g

Dissolve in 100 ml. H₂O and bring to pH 7.3 with 0.2 M NaOH. Add 6.84 % sucrose to the buffer used for washing and add 8.55% sucrose to the buffer used for ATP-Pb staining solutions.

ATP-Pb staining solution

Mix the solution just before use. Dissolve 10 mg. ATP (sigma) in 42 ml. tris-maleate buffer with 8.55% sucrose and prewarm to 37°C. Add 5 ml. 5% MgSO₄-7H₂O. Add, with agitation to prevent precipitation, 3 ml. 2% Pb(NO₃)₂.

Cacodylate buffered formaldehyde

Mix 100 ml. 0.2 M cacodylate buffer (pH 7.4) and 4 g paraformaldehyde. Heat the above mixture--avoid inhalation of fumes by carrying out this procedure in a well ventilated area, preferably a fume hood--to 70°C while stirring, until dissolved. Clarify with 2 drops 4% NaOH. Cool and store at 4°C.

REFERENCES

- (1) Snell G. D.: Inheritance in the house mouse; the linkage of short-ear, hairless and naked. *Genetics*, 16:42, 1931.
- (2) Montagna W., Chase, H. B. and Brown, P. J.: The skin of hairless mice. I. The formation of cysts and the distribution of lipids. *J. Invest. Derm.*, 19:83, 1952.
- (3) Orwin D. J. G., Chase H. B. and Silver A. F.: Catagen in the hairless mouse. *Am. J. Anat.*, 121:489, 1967.
- (4) Raknerud N., Hovig F. and Iverson O. H.: The ultrastructure of the interfollicular epidermis of the hairless (hr/hr) mouse. I. Basal and granular layer. *Virchows Arch. Abt. B. Zellpath.*, 8:206, 1971.
- (5) Breathnach A. S.: Observations on cytoplasmic organelles in Langerhans cells of human epidermis. *J. Anat.*, 98:265, 1964.
- (6) Wolff K. and Winkelmann R. K.: Quantitative studies on the Langerhans cell population of guinea-pig epidermis. *J. Invest. Dermatol.*, 48:504, 1967b.
- (7) MacKenzie I. and Squier C. A.: Cytochemical identification of ATPase-positive Langerhans cells in EDTA-separated sheets of mouse epidermis. *Br. J. Dermatol.*, 92:523, 1975.

- (8) Rowden G.: The Langerhans cell. CRC Crit. Rev. Immunol. 3:95, 1981.
- (9) Tsuji T., Sugai T. and Saito T.: Ultrastructure of three types of epidermal dendritic cells in hairless mice. J. Invest. Dermatol., 53:26, 1970.
- (10) Birbeck M. S., Breathnach A. S. and Everall J. S.: An electron microscopic study of basal melanocytes and high level clear cells (Langerhans cells) in vitiligo. J. Invest. Dermatol., 37:51, 1961.
- (11) Zelickson A. S. and Mottaz J. H.: Localization of gold chloride and adenosine triphosphatase in human Langerhans cells. J. Invest. Dermatol., 51:365, 1968.
- (12) Wolff K. and Winkelmann R. K.: Ultrastructural localization of nucleoside triphosphatase in Langerhans cells. J. Invest. Dermatol., 48:50, 1967a.
- (13) Rowden G, Lewis M. G. and Sullivan A. J.: Ia antigen expression on human epidermal Langerhans cells. Nature (London), 268:248, 1977.
- (14) Klareskog L., Tjernlund U. M., Forsum U. and Peterson P. A.: Epidermal Langerhans cells express Ia antigen. Nature (London), 26:248, 1977.
- (15) Tamaki K., Stingl G., Sachs D. H. and Katz S. I.: Ia antigens in mouse skin are predominately expressed on Langerhans cells. J. Immunol., 123:784, 1979.

- (16) Rowden G., Phillips T. M. and Delovitch T. L.:
Expression of Ia antigens by murine keratinizing
epithelial Langerhans cells. Immunogenetics,
7:465, 1978.
- (17) Fithian E., Kung P., Goldstein G., Rubenfeld M.,
Fenoglio C. and Edelson R.: Reactivity of
Langerhans cells with hybridoma antibody. Proc.
Natl. Acad. Sci. (USA), 78:2541, 1981.
- (18) Stingl G., Wolff-Shreiner E. C., Pichler W. J.,
Gschnait F. and Knapp W.: Epidermal Langerhans
cells bear Fc and C3 receptors. Nature (London),
268:245, 1977.
- (19) Giacometti L. and Montagna W.: Langerhans cells: uptake
of tritiated thymidine. Science, 157:439, 1967.
- (20) MacKenzie I. C.: Labelling of murine epidermal
Langerhans cells with H-thymidine. Am. J. Anat.,
144:127, 1975.
- (21) Katz S. I., Tamaki K. and Sacks D. H.: Epidermal
Langerhans cells are derived from cells
originating in bone marrow. Nature, 282:324, 1979.
- (22) Frelinger J. G., Hood L., Hill S. and Frelinger J. A.:
Mouse epidermal Ia molecules have a bone marrow
origin. Nature, 282:321, 1979.

- (23) Stingl G., Katz S. I., Shevach E. M., Rosenthal A. S. and Green I.: Analogous functions of macrophages and Langerhans cells in the initiation of the immune response. *J. Invest. Dermatol.*, 71:59, 1978.
- (24) Stingl G., Katz S. I., Green I. and Shevach E. M.: The functional role of Langerhans cells. *J. Invest. Dermatol.*, 74:325, 1980.
- (25) Silberberg I.: Apposition of mononuclear cells to Langerhans cells in contact allergic reactions. *Acta Dermatovenereol (Stockholm)*, 53:1, 1973.
- (26) Shelly W. B. and Juhlin L.: A reticulo-epithelial system: cutaneous trap for antigens. *Trans. Assoc. Am. Physicians*. 89:245, 1976.
- (27) Rowden G., Lewis M. G. and Phillips T. M.: Dendritic cells of the human epidermis: immuno-electron microscopic studies of Ia antigen reactivity. In: Sturgess J. M. (ed.) *Electron Microscopy 1978*. p. 644-645.
- (28) Quevedo W. C. and Smith J.: Electron microscopic observations on the postnatal "loss" of interfollicular epidermal melanocytes in mice. *J. Cell Biol.*, 39:108a, 1968.

- (29) Wolff K. and Winkelmann R. K.: The influence of ultraviolet light on the Langerhans cell population and its hydrolytic enzymes in guinea-pigs. *J. Invest. Dermatol.*, 48:531, 1967c.
- (30) Breathnach A. S.: Embryology of human skin. A review of ultrastructural studies. *J. Invest. Dermatol.*, 57:133, 1971.
- (31) Kurosumi K., Kurosumi H. and Inoue K.: Morphological and morphometric studies with the electron microscope on the Merkel cells and associated nerve terminals of normal and denervated skin. *Arch. Histol. Jap.*, 42:243, 1979.
- (32) Schmid R. W. and Reilly C. N.: New complexon for titration of calcium in the presence of magnesium. *Anal. Chem.*, 29:264, 1957.
- (33) Scaletta L. J. and MacCallum D. K.: A fine structural study of divalent cation-mediated union with connective tissue in human oral mucosa. *Am. J. Anat.*, 133:431, 1972.
- (34) Drzewiecki K. T. and Kjaergaard J.: Scanning electron microscopy of melanocytes in normal human epidermis. In: Bierrin F. (ed.), *Proceedings of the ninth congress of the nordic society for cell biology*. Odense university press, Denmark. p. 171-176, 1975.

- (35) Briggaman R. A. and Wheeler C. E.: The epidermal-dermal junction. *J. Invest. Dermatol.*, 65:71, 1975.
- (36) Juhlin L. and Shelley W. B.: New staining Techniques for the Langerhans cell. *Acta Derm. Venereol.*, 57:289, 1977.
- (37) Luft J. H.: Ruthenium red and violet. I Chemistry, purification, methods of use for electron microscopy and mechanism of action. *Anat. Rec.*, 171:347, 1971.
- (38) Luft J. H.: Ruthenium red and violet. II Fine structural localization in animal tissues. *Anat. Rec.*, 171:369, 1971.
- (39) Feria-Velasco A. and Arauz-Contreras J.: Ruthenium red as a ligand of osmium for examining uncoated material in the scanning electron microscope. *Proceedings of the electron microscope society of america*. p. 554-555, 1977.
- (40) Babai F.: An ultrastructural method for the study of cell viability using ruthenium red. In: Sturgess J. M. (ed.), *Electron Microscopy 1978*. p. 304-305.
- (41) Ruddick J. A.: Toxicology, metabolism and biochemistry of 1,2-propanediol. *Toxicology and Applied Pharmacology*, 21:102, 1972.
- (42) Ostrenga J., Haleblan J., Poulsen B., Ferrel B., Mueller N. and Shastri S.: Vehicle design for a new topical steroid, fluocinide. *J. Invest. Dermatol.*, 56:392, 1971.

- (43) Stoughton R. B.: Penetration of drugs through the skin.
Dermatologica, 152(suppl. 1):27, 1971.
- (44) Scheuplain R. J., Blank I. H., Brauner G. J. and
MacFarlane D. J.: Percutaneous absorption of steroids.
J. Invest. Dermatol., 52:63, 1969.
- (45) Brown W. R. and Habowsky J. E. J.: Comparative
ultrastructure and cytochemistry of epidermal
responses to tape stripping, ethanol and vitamin A
acid in hairless mice. *J. Invest. Dermatol.*, 73:203,
1979.
- (46) Goodman D. S.: Vitamin A and retinoids: Recent advances.
Fed. Amer. Soc. Exp. Biol., 38:2501, 1979.
- (47) McCollum E. V. and Davis M.: The necessity of certain
lipins in the diet during growth. *J. Biol. Chem.*,
15:167, 1913.
- (48) McCollum E. V., Simmonds S. and Pitz W.: The relation of
the unidentified dietary factors, the fat soluble A,
and water soluble B, of the diet to the growth
promoting properties of milk. *J. Biol. Chem.*, 27:33,
1916.
- (49) DeLuca H. F. and Zile M.: Aspects of teratology of vitamin
A acid (B-all-trans retinoic acid). *Acta. Dermatovenor*
(Stockholm), suppl. 74, 1975.

- (50) Christophers E. and Wolff H. H.: Effects of vitamin A acid on skin: In vivo and in vitro studies. Acta dermatovenor (Stockholm), suppl. 74, 1975.
- (51) Anzano M. A., Lamb A. J. and Olson J. A.: Growth, appetite, sequence of pathological signs and survival following the induction of rapid synchronous vitamin A deficiency in the rat. J. Nutr., 109:1419, 1979.
- (52) DeLuca H. F.: Retinoic acid metabolism. Fed. Amer. Soc. Exp. Biol., 38:2501, 1979.
- (53) Dowling J. E. and Wald G.: The biological function of vitamin A acid. Proc. Natl. Acad. Sci., USA, 46:587, 1960.
- (54) Roberts A. B. and Frolich C. A.: Recent advances in the in vivo and in vitro metabolism of retinoic acid. Fed. Amer. Soc. Exp. Biol., 38:2524, 1979.
- (55) Frolich C. A.: The in vitro and in vivo metabolism of all-trans- and 13-cis-retinoic acid in the hamster. Proc. N. Y. Acad. Sci., 359:37, 1980.
- (56) Roberts A. B.: Microsomal oxidation of retinoic acid in hamster liver, intestine and testis. Proc. N. Y. Acad. Sci., 359:45, 1980.
- (57) Roberts A. B., Lamb L. C. and Sporn M. B.: Metabolism of all-trans-retinoic acid in hamster liver microsomes: Oxidation of 4-hydroxy- to 4-keto-retinoic acid. Arch. Biochem. Biophys., 199:374, 1980.

- (58) Rask L., Annundi H., Ronne H., Erikson U., Bohme J. and Peterson P. A.: Structural and functional analysis of vitamin A-binding proteins. *Proc. N. Y. Acad. Sci.*, 359:79, 1980.
- (59) Goodman D. S.: Retinoid-binding proteins in plasma and in cells. *Proc. N. Y. Acad. Sci.*, 359:69, 1980.
- (60) Chytil F. and Ong D. E.: Cellular retinol- and retinoic acid-binding proteins in vitamin A action. *Fed. Amer. Soc. Exp. Biol.*, 38:2510, 1979.
- (61) Smith J. E., Milch P. O., Muto J. and Goodman D. S.: The plasma transport of retinoic acid in the rat. *Biochem. J.*, 132:821, 1973.
- (62) Chytil F. and Ong D. E.: Mediation of retinoic acid-induced growth and anti-tumour activity. *Nature (London)*, 260:49, 1976.
- (63) O'Malley W. B. and Shraeder W. F.: The receptors of steroid hormones. *Science*, 234:32, 1976.
- (64) DeLuca L., Pangala B. V., Wlodzimierz S. and Adamo S.: Biosynthesis of phosphoryl and glycosyl phosphoryl derivatives of vitamin A in biological membranes. *Fed. Amer. Soc. Exp. Biol.*, 38:2535, 1979.
- (65) Wolff G., Kiorpes T. C., Masushige S., Shreiber J. B., Smith M. J. and Anderson R. S.: Recent evidence for the participation of vitamin A in glycoprotein synthesis. *Fed. Amer. Soc. Exp. Biol.*, 38:2540, 1979.

- (66) Shapiro S. S. and Mott J.: Modulation of glucosaminoglycan biosynthesis by retinoids. Proc. N. Y. Acad. Sci., 359:306, 1980.
- (67) Shidoji Y., Sasak W., Silverman-Jones and DeLuca L.: Recent studies on the involvement of retinyl phosphate as a carrier of mannose in biological membranes. Proc. N. Y. Acad. Sci., 359:345, 1980.
- (68) Lehninger A. L.: Biochemistry. Worth publishers inc., New York, 1976.
- (69) Roseman S.: The synthesis of complex carbohydrates by multiglycosyl transferase systems and their potential function in adhesion. Chem. Phys. Lipids, 5:270, 1970.
- (70) Fell H. B. and Mellanby E.: Metaplasia produced in cultures of chick ectoderm by high vitamin A. J. Physiol., 119:470, 1953.
- (71) Sweeny P. R. and Hardy M. H.: Ciliated and secretory epidermis produced from embryonic mammalian skin organ culture by vitamin A. Anat. Rec., 185:93, 1975.
- (72) Pelc S. R. and Fell H. B.: The effect of excess vitamin A on the uptake of labelled compounds by embryonic skin in organ culture. Exp. Cell Res, 19:99, 1960.
- (73) Barnett M. L. and Szabo G.: Effect of vitamin A on epithelial morphogenesis in vitro. Exp. Cell Res., 76:118, 1973.
- (74) Christophers E. and Wolff H. H.: Differential formation of desmosomes and hemidesmosomes in epidermal cell

cultures treated with retinoic acid. *Nature* (London), 256:209, 1975.

- (75) Wilkinson D.: Effect of vitamin A acid on the growth of keratinocytes in culture. *Arch. Dermatol. Res.*, 263:75, 1978.
- (76) Hof H. and Emmerling P.: Stimulation of cell mediated resistance in mice to infection with *Listeria monocytogenes* by vitamin A. *Ann. Immunol.*, 130c:587, 1979.
- (77) Kaidby K. H., Kligman A. M. and Yoshida: Effects of intensive application of retinoic acid on human skin. *Br. J. Dermatol.*, 92:693, 1974.
- (78) Wolff H. H., Christophers E. and Braun-Falco O.: Beeinflussung der epidermalen ausdifferenzierung durch vitamin A-saure. *Arch. Klin. Exp. Dermatol.*, 237:774, 1970.
- (79) Zil J. S.: Vitamin A acid effects on epidermal mitotic activity, thickness and cellularity in the hairless mouse. *J. Invest. Dermatol.*, 59:228, 1972.
- (80) Sherman B. S.: The effect of vitamin A on epithelial mitosis in vitro and in vivo. *J. Invest. Dermatol.*, 37:469, 1961.
- (81) Mizumoto T., Aoyagi T., Ohkawara A. and Muira Y.: The action of topical vitamin A acid on normal epidermis and non-involved epidermis of psoriatics: A morphological and enzymatic study. *J. Dermatol.*, 1:32, 1974.

- (82) Bollag W.: From vitamin A to retinoids in experimental and clinical oncology: Achievements, failures and outlook. Proc. N. Y. Acad. Sci., 359:9, 1980.
- (83) Tsuji T., Sugai T. and Saito T.: Ultrastructure of three types of epidermal dendritic cells in hairless mice. J. Invest. Dermatol., 53:332, 1969.
- (84) Reinharz E. L. and Schlossman S. F.: The characterization and function of human immunoregulatory T lymphocyte subsets. Immunology Today, April 1981.
- (85) Bergstresser P. R., Fletcher C. R. and Streilein W. S.: Surface densities of Langerhans cells in relation to rodent epidermal sites with special immunologic properties. J. Invest. Dermatol., 74:77, 1980.
- (86) Schweizer J. and Marks F.: A developmental study of the distribution and frequency of Langerhans cells in relation to formation of patterning in mouse tail epidermis. J. Invest. Dermatol., 69:201, 1977.
- (87) Reams W. M. and Tomkins S. P.: A developmental study of murine epidermal Langerhans cells. Develop. Biol., 31:114, 1973.
- (88) Toews G. B., Bergstresser P. R., Streilein J. W. and Sullivan S.: Epidermal Langerhans cell density determines whether contact hypersensitivity or unresponsiveness follows skin painting with DNFB. J. Immunol., 124:445, 1980.

- (89) Streilein J. W., Toews G. T., Gilliam J. N. and Bergstresser P. R.: Tolerance or hypersensitivity to 2,4-dinitro-1-fluorobenzene: The role of Langerhans cell density within epidermis. *J. Invest. Dermatol.*, 74:319, 1980.
- (90) Rowden G.: Personal communication.
- (91) Papa C. M. and Farber B.: Direct scanning electron microscopy of human skin. *Arch. Dermatol.*, 104:262, 1971.
- (92) McCarthy D. T. and Habowsky J. E. J.: Structural variability of the dermo-epidermal interface of the skin of the human foot as related to function. *J. Amer. Pod.*, 65:451, 1975.
- (93) Odland G. F. and Reed T. H.: Epidermis. In: Zelickson A. S. (ed.), *Ultrastructure of Normal and Abnormal Skin*. Philadelphia, Lea and Febinger. 1967, p. 54-75.
- (94) Elias P. M. and Friend D. S.: The permeability barrier in mammalian epidermis. *J. Cell Biol.*, 65:180, 1975.
- (95) Lavker R. M.: Membrane coating granules: The fate of the discharged lamellae. *J. Ultrastr. Res.*, 55:79, 1976.
- (96) Prutkin L.: Mucous metaplasia and gap junctions in the vitamin A acid-treated tumour, keratoacanthoma. *Cancer Res.*, 35:364, 1975.
- (97) Zbinden G.: Pharmacology of vitamin A acid (B-all-trans retinoic acid). *Acta. Dermatovenor (Stockholm)*, suppl. 74, 1975.

- (98) Nix T. E.: Ultraviolet-induced changes in epidermis. In: Zelickson A. S. (ed.) *Ultrastructure of Normal and Abnormal Skin*, Philadelphia, Lea and Febiger. 1967, p.304.
- (99) Bradfield J. R. G.: Glycogen of vertebrate epidermis. *Nature (London)*, 167:40, 1951.
- (100) Baker K. W.: Preliminary results; research in progress.
- (101) Argyris T. S.: Glycogen in the epidermis of mice painted with methylcholanthrene. *J. Natl. Cancer Inst.*, 12:1159, 1952.
- (102) Matoltsy A. G. and Matoltsy M. N.: Cytoplasmic droplets of pathologic horny cells. *J. Invest. Dermatol.*, 38:323, 1962.
- (103) Brody I.: The ultrastructure of the epidermis in psoriasis vulgaris as revealed by electron microscopy. 3. Stratum intermedium in parakeratosis without keratohyalin. *J. Ultrastr. Res.*, 6:341, 1962.
- (104) Brody I.: The ultrastructure of the epidermis in psoriasis vulgaris as revealed by electron microscopy. 4. Stratum corneum in parakeratosis without keratohyalin. *J. Ultrastr. Res.*, 6:354, 1962.
- (105) Brody I.: The ultrastructure of the epidermis in psoriasis vulgaris as revealed by electron microscopy. 7. The stratum corneum in hyperkeratosis. *J. Ultrastr. Res.*, 8:595, 1963.

- (106) Frei J. V. and Sheldon H.: Corpus intra cristam: A dense body within mitochondria of cells in hyperplastic mouse epidermis. J. Biophys. Biochem. Cytol., 11:724, 1961.
- (107) Rupec M. and Bruhl R.: On the question of the ultrastructure and composition of corpus intra cristam after local methylcholanthrene application. J. Ultrasstr. Res., 54:388, 1976.
- (108) Kakefuda T., Roberts E. and Suntzeff V.: Electron microscopic study of methylcholanthrene-induced epidermal carcinogenesis in mice: mitochondrial dense bodies and intracisternal A particles. Cancer Res., 3:1011, 1970.
- (109) Tarin D. J.: Sequential electron microscopical study of experimental mouse skin carcinogenesis. Int. J. Cancer, 2:195, 1967.
- (110) Potten C. S. and Allen T. D.: The fine structure and cell kinetics of mouse epidermis after wounding. J. Cell Sci., 17:413, 1975.

VITA AUCTORIS

Born: May 25, 1952. Windsor, Ontario, Canada. Son of Mr. and
Mrs. Bernard Baker

Primary Education:

Central Public School, Windsor, Ontario. 1958-1966.

Secondary Education:

Vincent Massey Secondary School and Centennial
Secondary School, Windsor, Ontario. 1966-1969,
1970-1972.

University Education:

University of Windsor, Windsor, Ontario. 1973-1975,
1976-1978. (BSc)